

# Contextual Budget Allocation for Food Rescue Volunteer Engagement

Ariana Tang<sup>1</sup>, Naveen Raman<sup>2</sup>, Fei Fang<sup>2</sup> and Ryan Shi<sup>3</sup>

<sup>1</sup>Shanghai University of Finance and Economics

<sup>2</sup>Carnegie Mellon University

<sup>3</sup>University of Pittsburgh

ariana.tang@stu.sufe.edu.cn, {naveenr, feifang}@cmu.edu, ryanshi@pitt.edu

## Abstract

1 Volunteer-based food rescue platforms tackle food  
2 waste by matching surplus food to communities in  
3 need. These platforms face the dual problem of  
4 maintaining volunteer engagement and maximizing  
5 the food rescued. Existing algorithms to improve  
6 volunteer engagement exacerbate geographical dis-  
7 parities, leaving some communities systematically  
8 disadvantaged. We address this issue by extending  
9 restless multi-armed bandits, a model of decision-  
10 making which allows for stateful arms, to incorpo-  
11 rate context-dependent budget allocation. By do-  
12 ing so, we can allocate higher budgets to commu-  
13 nities with lower match rates, thereby alleviating  
14 geographical disparities. To tackle this problem,  
15 we develop an empirically fast heuristic algorithm.  
16 Because such an algorithm can achieve a poor ap-  
17 proximation when active volunteers are scarce, we  
18 design the Mitosis algorithm, which is guaranteed  
19 to compute the optimal budget allocation. Em-  
20 pirically, we demonstrate that our algorithms out-  
21 perform baselines on both synthetic and real-world  
22 food rescue datasets, and show how our algorithm  
23 achieves geographical fairness in food rescue.

## 1 Introduction

25 The world wastes up to 40% of our food globally, translating  
26 to over 1.3 billion tons annually, while 1 in 7 people strug-  
27 gle to secure enough food every day [Coleman-Jensen *et al.*,  
28 2018; Conrad *et al.*, 2018]. With their appearance in over  
29 100 cities worldwide, food rescue platforms (FRP) receive  
30 safe, edible food donations from businesses like restaurants  
31 (“donors”) and distribute them to organizations serving low-  
32 resource communities (“recipients”). Our partner organiza-  
33 tion, Food Rescue X<sup>1</sup>, is a large FRP with operations in over  
34 25 different cities across the US. FRPs are able to scale due  
35 to volunteers, who transport food from donors to recipients.  
36 Essentially, volunteers claim “rescues” from an FRP’s mobile  
37 app. After claiming the rescue, the app instructs them where  
38 to pick up and drop off the donation.

<sup>1</sup>Real name blinded.

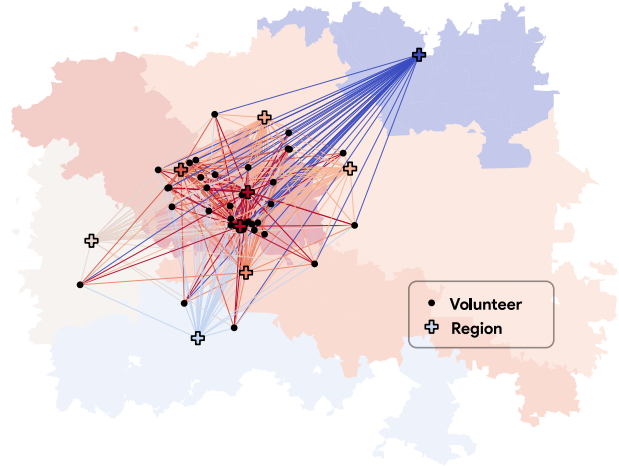


Figure 1: The picture shows volunteers and donation regions in real food rescue database. Region color indicates the richness of volunteer resource. Connected lines indicates how volunteers and real-time donation tasks are matched by food-rescue platforms.

39 The inclusion of volunteers in FRPs brings about inherent  
40 uncertainty due to changing volunteer behavior. Volunteer  
41 engagement is critical to FRP success, so FRPs have an ur-  
42 gent need to engage their volunteers while maximizing the  
43 amount of food rescued. A few studies have developed al-  
44 gorithms to improve volunteer engagement on FRPs by dy-  
45 namically notifying volunteers about rescue trips [Shi *et al.*,  
46 2021, 2024; Raman *et al.*, 2024]. However Shi *et al.* [2021]  
47 showed that such algorithms can backfire because they result  
48 in severe geographical disparity in food rescue outcomes. In  
49 some regions such as downtown, the algorithm enjoyed al-  
50 most 90% completion rate, while in some outer suburbs, the  
51 completion rate dropped to 40%.

52 In our work, we study how to maintain volunteer engage-  
53 ment while combatting geographical disparities. The chal-  
54 lenge is that volunteer behaviors evolve over time in response  
55 to notification patterns. To tackle this issue, we model food  
56 rescue volunteer engagement as a restless multi-armed bandit  
57 (RMAB) problem, a common model for online resource allo-  
58 cation [Mate *et al.*, 2020; Raman *et al.*, 2024]. We extend this  
59 model to incorporate geographical disparities with a *context*,

60 which corresponds to geographic information for each rescue  
 61 trip. We then set notification quotas for different regions so  
 62 certain regions with scarce volunteers have higher budgets.  
 63 Such an approach allows for flexibility in notifications with-  
 64 out sacrificing overall performance.

65 We make the following contributions: (1) We propose the  
 66 *Contextual Budget Bandit* problem, which extends RMABs to  
 67 situations with context-dependent budget allocations. Such a  
 68 problem is motivated by applications in food rescue, but can  
 69 also model problems in domains such as digital farming and  
 70 peer review (see Appendix E). (2) We develop the COcc, a  
 71 fast, empirically approximation algorithm which provides an  
 72 upper bound to Contextual Budget Bandit. We characterize  
 73 cases where it fails with a constant factor; (3) We design the  
 74 Mitosis algorithm which is guaranteed to compute the opti-  
 75 mal budget allocation; and (4) We empirically demonstrate  
 76 that our algorithms improve upon baselines with synthetic  
 77 and real-world food rescue datasets.

## 78 2 Preliminary Background

79 A Restless Multi-Armed Bandit (RMAB) is defined by:

$$\langle N, \mathcal{S}, \mathcal{A}, \{r_i\}_{i \in [N]}, \{P_i\}_{i \in [N]} \rangle.$$

Each arm  $i \in [N] := \{1, 2, \dots, N\}$  is an independent  
 Markov Decision Process, with state space  $\mathcal{S}_i = \{0, 1\}$  and  
 binary action space  $\mathcal{A}_i = \{0, 1\}$ . Action 0 corresponds  
 to idling the arm while action 1 corresponds to pulling the  
 arm. The reward function for each arm  $r_i : \mathcal{S}_i \times \mathcal{A}_i \rightarrow \mathbb{R}$   
 maps state-action pairs to a reward.  $P_i$  is the transition ker-  
 nel for each arm  $i$ . The overall system state at time  $t$  is  
 $\mathbf{s}^t = (s_1^t, s_2^t, \dots, s_N^t)$ , and the decision maker selects action  
 $\mathbf{a}^t = (a_1^t, a_2^t, \dots, a_N^t)$  subject to a budget constraint:

$$\sum_{i \in [N]} a_i^t \leq B, \quad \forall t = 1, 2, \dots,$$

80 which limits the number of arms that can be pulled in every  
 81 time step. The objective is to design a policy that maps the  
 82 current state  $\mathbf{s}^t$  to an action vector  $\mathbf{a}^t$  that maximizes the av-  
 83 erage reward over all arms and over an infinite time horizon.

A widely-adopted approach for tackling the computational  
 complexity inherent in RMABs is the Whittle Index Policy.  
 The *Whittle Index* for each arm  $i$ 's state  $s_i \in \mathcal{S}_i$  is:

$$w_i(s_i) = \min_w \{w | Q_{i,w}(s_i, 0) = Q_{i,w}(s_i, 1)\},$$

$$Q_{i,w}(s_i, a_i) = -wa_i + r_i(s_i, a_i) + \gamma \sum_{s'} P_i[s_i, a_i, s'] V_{i,w}(s')$$

$$V_{i,w}(s') = \max_a Q_{i,w}(s', a)$$

85  $Q_{i,w}(s_i, a_i)$  represents the expected future reward for play-  
 86 ing action  $a_i$ , given a penalty  $w$  for pulling an arm. Under  
 87 the crucial condition of **indexability**—which requires that the  
 88 set of states where it is optimal to activate an arm decreases  
 89 monotonically as the subsidy  $w$  increases—the Whittle index  
 90 is well-defined and interpretable as the marginal value of ac-  
 91 tivating an arm. At each time step, the *Whittle Index Policy*  
 92 pulls the  $B$  arms with the highest Whittle Indices. In this

way, it decouples the multi-armed problem into a collection  
 of single-arm problems. The Whittle index policy is asymp-  
 totically optimal under regularity conditions as the number of  
 arms goes to infinity [Gittins *et al.*, 2011].

## 3 Contextual Budget Bandit

Because traditional methods to maintain volunteer engage-  
 ment can lead to geographical disparity [Shi *et al.*, 2021], we  
 pursue an intuitive solution where we allocate different notifi-  
 cation budget to different regions. To do this, we need to aug-  
 ment the standard RMAB model with variability in transition  
 and reward across time, and the flexibility to adjust budget  
 accordingly. In this section, we will introduce the Contextual  
 Budget Bandit model and multiple algorithms for it.

### 3.1 The Contextual Budget Bandit Model

A Contextual Budget Bandit (CBB) is defined by the tuple

$$\langle N, \mathcal{S}, \mathcal{A}, K, \{r_i^k\}_{i \in [N], k \in [K]}, \{P_i^k\}_{i \in [N], k \in [K]}, \mathcal{F} \rangle.$$

Departing from the standard RMAB model, we introduce the  
 $[K] = \{1, 2, \dots, K\}$  (finite) **contexts**. A Borel measure  $\mathcal{F}$   
 on  $[K]$  specifies the distribution over these contexts, which  
 is known by the decision maker. At each time step, a new  
 context is sampled with respect to  $\mathcal{F}$  and globally applies  
 to all arms.  $r_i^k, P_i^k, \forall k \in [K]$  are the reward function and  
 the transition probability kernels *specific to context*  $k$ .  $\mathcal{F}$  and  
 $\{P_i^k\}_{i \in [N], k \in [K]}$  are independent.

**Definition 3.1** (Context Specific Budget Constraint). A pol-  
 icy is said to satisfy *Context Specific Budget Constraint* if the  
 number of arms pulled at each time step is constrained by a  
 budget  $B_k$  contingent on context, while the expected budget  
 usage is still bounded by  $B$ :

$$\sum_{i \in [N]} a_i^t \mathbb{I}(k^t = k) \leq B_k, \quad \forall t, k, \quad \text{and} \quad \mathbb{E}_{k \sim \mathcal{F}} B_k \leq B.$$

A policy  $\pi$  for CBB (i) pre-specifies budget allocation  $\vec{B}$   
 and (ii) maps the current states of all arms and the context  $k$   
 to an action vector:  $\pi : \{\mathcal{S}, [K]\} \mapsto \mathcal{A}$ . The objective is then  
 to maximize the expected average reward across timesteps,  
 where the expectation is taken over contexts:

$$\lim_{T \rightarrow \infty} \mathbb{E}_{\mathbf{a} \sim \pi, k \sim \mathcal{F}} \left[ \frac{1}{T} \sum_{t=1}^T \sum_{i \in [N]} r_i^k(s_i^t, a_i^t) \right].$$

The Whittle Index Policy for standard RMAB satisfies the  
 above Context Specific Budget Constraint (Definition 3.1),  
 because it uses a uniform budget for each context  $\vec{B} =$   
 $(B, \dots, B)$ . However, its performance can be arbitrarily bad:

**Theorem 1.** For a CBB, denote the Whittle Index Policy's  
 reward as  $\mathcal{R}^{\text{VanillaWhittle}}$ , and the optimal policy that satisfies  
 context-specific budget constraint as  $\mathcal{R}^{\text{ContextOpt}}$ . There exists  
 an instance where,

$$\frac{\mathcal{R}^{\text{ContextOpt}}}{\mathcal{R}^{\text{VanillaWhittle}}} \rightarrow \infty, \quad \text{as } N \rightarrow \infty.$$

## 120 3.2 Contextual Occupancy Index (COcc) Policy

121 Having established that the vanilla Whittle Index policy could  
 122 perform arbitrarily bad in CBB, we now develop an efficient  
 123 heuristic algorithm, the COcc. First, we introduce the *occu-*  
 124 *pancy measure*.

**Definition 3.2.** The occupancy measure  $\mu$  of a (possibly ran-  
 domized) policy  $\pi$  in CBB is the average visitation probabili-  
 ty to a state-action-context tuple  $(s, a; k)$ :

$$\mu_i(s, a; k) := \mathbf{Pr} [s_i = s, a_i = a; k], \forall i \in [N].$$

125 We next show how we can formulate the problem of max-  
 126 imizing the stationary reward as a linear program (LP) over  
 127 occupancy measures.

128 **Definition 3.3.** For a given contextual-RMAB instance, its  
 129 *occupancy-measure LP* is

$$\max_{\mu} \sum_{i \in [N]} \sum_{k \in [K]} \sum_{s_i, a_i} \mu_i(s_i, a_i; k) r_i(s_i, a_i; k) \quad (1)$$

$$s.t. f_k \left[ \sum_{k \in [K]} \sum_{s_i, a_i} P[s_i \rightarrow s'_i | a_i, k] \mu_i(s_i, a_i; k) \right] \quad (2)$$

$$= \sum_{a_i} \mu_i(s'_i, a_i; k'), \forall k', s'_i, i \quad (3)$$

$$\sum_{k \in [K]} \sum_{a_i, s_i} \mu_i(s_i, a_i; k) = 1, \forall i \in [N] \quad (4)$$

$$\sum_{k \in [K]} \sum_i \sum_{s_i} \mu_i(s_i, 1; k) \leq B \quad (5)$$

$$\mu_i(s_i, a_i, k) \geq 0, \forall i, s_i, a_i, k. \quad (6)$$

**Definition 3.4** (Adapted from [Xiong *et al.*, 2022]). Given  
 the optimal solution  $\mu^*(\cdot, \cdot; k)$  to the occupancy-measure LP,  
 the Contextual Occupancy **Soft Budget** Policy  $\pi^{\text{soft}}$  pulls an  
 arm  $i$  in state  $s_i$  and context with probability  $\chi_i^*(s_i, k)$ , where

$$\chi_i^*(s_i, k) = \frac{\mu_i^*(s_i, 1; k)}{\mu_i^*(s_i, 0; k) + \mu_i^*(s_i, 1; k)}.$$

130 The Contextual Occupancy **Soft Budget** Policy is not  
 131 immediately applicable because the budget constraint in  
 132 Equation 5 is only a relaxed version. Thus, denoting the  
 133 occupancy-measure LP's objective value as  $\bar{\mathcal{R}}$ , we have

$$\mathcal{R}^{\text{VanillaWhittle}} \leq \mathcal{R}^{\text{ContextOpt}} \leq \bar{\mathcal{R}}. \quad (7)$$

The Contextual Occupancy **Soft Budget** Policy can  
 achieve a high reward because it can shift budget across time  
 — by saving up budget at bad context and using them when  
 context is good. Guided by this insight, we introduce the Con-  
 textual Occupancy Index Policy (COcc) that mimics the Con-  
 textual Occupancy **Soft Budget** Policy, but further satisfies a  
 context-dependent budget constraint for a set of budgets  $\vec{B}$ :

$$B_k = \frac{1}{f_k} \sum_{i, s_i} \mu_i^*(s_i, 1; k), \quad \forall k$$

134 where  $\mu^*$  are optimal solutions from occupancy-measure LP.

Given a context  $k$ , to determine which arms to pull,  
 we tend to the dual of the occupancy-measure LP<sup>2</sup>. Let  
 $V_i(s_i, k), \forall i, s_i, k$  be the Lagrangian for constraint (2, 3). Let  
 $\nu_i, \forall i$  be the Lagrangian multiplier for (4), and  $\rho$  for (5). The  
 dual of the occupancy-measure LP is

$$\min_{V, \rho, \nu} \sum_{i \in [N]} \nu_i + \rho B \quad (8)$$

$$s.t. V_i(s_i, k) + \nu_i \geq r_i(s_i, a_i; k) - \rho \mathbb{1}\{a_i = 1\} \quad (9)$$

$$+ \sum_{s'_i, k'} V_i(s'_i, k') P[s_i \rightarrow s'_i | a_i, k], \forall s_i, a_i, k \quad (10)$$

$$\rho \geq 0 \quad (11)$$

The solution of the dual of the occupancy-measure LP par-  
 titions every arm's state-context pair  $(s_i, k)$  into three sets,  
 $E_0, E_1$  and  $E_{01}$  where respectively, the optimal action is pos-  
 itive, negative or some randomization.<sup>3</sup>

The optimal Lagrangian multiplier  $\rho^*$  in the dual problem  
 can be interpreted as an extra cost for taking the positive ac-  
 tion ( $a_i = 1$ ). Under indexability, as the cost  $\rho^*$  increases, the  
 set of state-context  $(s_i, k)$  in which negative action is optimal  
 ( $E_0$ ) increases monotonically. Thus, we define the *Context-*  
*tual Whittle Index* for each state-context pair  $(s_i, k)$  of each  
 arm, denoted as  $\rho_i^*(s_i, k)$ , as the least value of the cost  $\rho$  such  
 that negative action is optimal:

$$\rho_i^*(s_i, k) := \sup\{\rho : (s_i, k) \in E_0\}.$$

With this, we are ready to formally define our COcc. 144

**Definition 3.5** (The **Contextual Occupancy Index** (COcc)  
 Policy). At each time step, given context  $k$ , the COcc pulls  
 top- $B_k$  arms that have the highest positive Contextual Whittle  
 Index, where

$$B_k = \frac{1}{f_k} \sum_{i, s_i} \mu_i^*(s_i, 1; k),$$

with  $\mu^*$  being optimal solutions from occupancy-measure LP. 145

Standard RMAB problems correspond to  $B_k$  being the  
 same across all  $k$ , and in such a situation, the COcc is equiv-  
 alent to the Whittle Index Policy, and is asymptotically opti-  
 mal.<sup>4</sup> However, the COcc is not optimal for CBB: 149

**Theorem 2.** The COcc's asymptotic approximation ratio  
 compared to  $\mathcal{R}^{\text{ContextOpt}}$  is bounded above by  $\frac{5}{6}$ . 151

The source of the suboptimality comes from when there are  
 more than one contexts. The proof in Appendix C presents an  
 original mathematical framework for asymptotic analysis. 154

<sup>2</sup>detail of obtaining the dual is in Appendix B

<sup>3</sup>To avoid uninteresting pathologies, assume every pure policy  
 gives rise to a Markov chain with one recurrent class, then the ran-  
 domization set  $E_{01}$  need not contain more than one object [Gittins  
*et al.*, 2011].

<sup>4</sup>The asymptotic notion is usually to repeat all arms of an RMAB  
 instance infinitely, along with the budget for the same repeats.

### 3.3 Solving Optimal Budget Allocation Using Multi-Armed Bandit Algorithm

The COcc is suboptimal because it fails to determine the optimal budget allocation  $\vec{B}$ . Yet Contextual Whittle Index can still be used given a budget allocation.

**Definition 3.6.** A *Flexible Budget Allocation COcc* determines a budget allocation  $\vec{B} \in \mathcal{B}_0 := \{\vec{B} \in \mathbb{N}^K : \sum_{k=1}^K B_k \leq B\}$  given a total budget  $B$  and context probabilities  $\vec{f}$ , and pulls the  $B_k$  arms with the highest Contextual Whittle Index,  $\rho_i^*(s_i, k)$ .

Our goal is thus to find the optimal budget combination  $\vec{B}^*$  from the set of feasible budget allocations  $\mathcal{B}_0$ . Within the class of Flexible COcc(s), each budget allocation  $\vec{B}$ 's reward can be evaluated according to an Oracle function:

**Definition 3.7** (Oracle). The Oracle is a randomized simulation procedure that, given a budget allocation  $\vec{B} \in \mathbb{N}^K$ , runs the Flexible COcc using  $\vec{B}$  and returns the resulting reward. It has two parameters:

- Epochs: number of times simulation is repeated.
- T: the length of each simulation run.

Oracle gives us an estimate of policy performance, but it is slow. Meanwhile, we can obtain upperbounds for each budget allocation by inserting the following constraint into the occupancy-measure LP in Definition 3.3:

$$\frac{1}{f_k} \sum_{i, s_i} \mu_i(s_i, 1; k) = B_k \quad \forall B_k \in \vec{B}. \quad (12)$$

Given budget allocation  $\vec{B}$ , let  $\text{LP}(\vec{B})$  be the optimal value of occupancy-measure LP with constraint (12) inserted.

We next design two algorithms to find the best budget allocation by querying the Oracle and LP for a small subset of budget combinations, avoiding an exponential enumeration.

**The Branch And Bound Algorithm** Since  $\text{LP}(\vec{B}) \geq \text{Oracle}(\vec{B}), \forall \vec{B}$ , we design a Branch And Bound approach to efficiently search over the feasible solution space: it recursively splits the search region into smaller subregions and prunes subregions if its LP-based upperbound is lower than another's actual reward. Although Branch And Bound is still NP-hard in the worst case, it provides a systematic way to efficiently search. We provide the pseudocode (Algorithm 2) in appendix F.

**The Mitosis Algorithm** While Branch And Bound already cuts down the search tree dramatically compared to brute force search, it still calls too many costly Oracle evaluations on large-scale problems. To address this issue, we develop the following multi-armed bandit (MAB) framework which allows for more nuanced speed-accuracy trade-off for the evaluation of budget allocations:

**Definition 3.8** (MAB on top of Contextual-RMAB). We define an associated *Multi-Armed Bandit (MAB) problem* by identifying each arm with a vector  $\vec{B} \in \mathcal{B}_0$ . Pulling arm  $\vec{B}$  invokes the fast oracle  $\text{Oracle}_{\text{small}}(\vec{B})$  which returns a noisy reward  $r(\vec{B})$ .

A standard UCB-type algorithm maintains empirical statistics for each arm and computes an index that serves as an upper confidence bound on the arm's true reward. For each arm  $\vec{B}$  and time  $t$ , its upper-confidence-level index is given by

$$I_t(\vec{B}) := \hat{\mu}_t(\vec{B}) + f(N_t(\vec{B}), t),$$

where  $N_t(\vec{B})$  is the number of times arm  $\vec{B}$  has been selected and  $\hat{\mu}_t(\vec{B})$  the empirical mean reward from  $\vec{B}$ .  $f$  is chosen so that, with high probability,  $I_t(\vec{B})$  is an upper bound on the true mean reward  $\mu(\vec{B})$ . For example, the classical UCB1 algorithm sets

$$f(N_t(\vec{B}), t) = c \sqrt{\frac{\log t}{N_t(\vec{B})}}, \text{ for } c > 0.$$

**Addressing the Combinatorial Explosion with StemArm** Naively applying UCB to our setting would result in combinatorial explosion, so we incorporate the hierarchical tree structure from Branch And Bound to speed up our algorithms. A StemArm is a special arm that represents a *group* of candidate budget allocations. Instead of tracking every  $\vec{B}$ , we use StemArm to encapsulate less-promising budget allocations, which are grouped in polytope regions  $\mathcal{B}_m \subseteq \mathcal{B}_0$ . Formally,

$$\text{StemArm} = \cup_{m=1}^M \mathcal{B}_m.$$

When the StemArm is pulled, it splits out a most promising daughter arm:

$$\vec{B}_{\text{new}} := \arg \max_{\vec{B} \in \text{StemArm}} \text{LP}(\vec{B}),$$

And updates itself by partitioning the subregion that contains  $\vec{B}_{\text{new}}$  to exclude it from the StemArm:

Let  $\mathcal{B}^* :=$  the subregion containing  $\vec{B}_{\text{new}}$ .

**Split**  $\mathcal{B}^* = \{\vec{B}_{\text{new}}\} \cup \mathcal{B}_{\text{new}_1} \cup \mathcal{B}_{\text{new}_2}$ ,

**replace**  $\mathcal{B}^*$  with  $\mathcal{B}_{\text{new}_1}, \mathcal{B}_{\text{new}_2}$

Notice that all arms  $\vec{B} \in \text{StemArm}$  (before they are split out) are never pulled, so they have no empirical history for UCB value. Instead the StemArm's UCB index is assigned as the upperbound of all its arms  $\max_{\vec{B} \in \text{StemArm}} \text{LP}(\vec{B})$ . For convenience, denote it as  $\text{LP}(\text{StemArm})$ . Note that because every pull of the StemArm splits out the daughter arm with the highest LP value, the StemArm's UCB index  $\text{LP}(\text{StemArm})$  decreases during the Algorithm when it splits everytime.

Putting the MAB framework and StemArm together, the Mitosis algorithm operates as follows. We begin the MAB with the candidate arms containing only a StemArm, representing the entire feasible region  $\mathcal{B}_0$ . At each round, the algorithm selects from candidate arms (either a standard arm  $\vec{B}$  or a StemArm) with the highest UCB index. When a standard arm is pulled, we run  $r_t(\vec{B}) \leftarrow \text{Oracle}_{\text{small}}(\vec{B})$  to update its empirical statistics. When a StemArm is selected, it splits out

232 a new arm into candidate arms and we pull it. We present  
 233 pseudocode in Algorithm 1. The Mitosis algorithm is named  
 234 for how the StemArm ‘buds’ new arms progressively during  
 235 the algorithm, similar to cell division in mitosis.

236 Finally, we establish that our approach retains the no-regret  
 237 guarantees of classical MAB algorithms:

**Theorem 3.** [No-Regret of the Mitosis Algorithm] Let  $\mathcal{A}$  denote the set of arms that have been pulled. After running the algorithm for  $T$  rounds, the cumulative regret

$$R(T) \triangleq \sum_{t=1}^T (\mu^* - \mu_t)$$

satisfies

$$R(T) = \sum_{\vec{B} \in \mathcal{A}} \mathbb{E}[N_T(\vec{B})] \Delta(\vec{B}) = O\left(\sum_{\vec{B} \in \mathcal{A}} \frac{\log T}{\Delta(\vec{B})}\right),$$

238 which matches the UCB1 regret bound.

239 To sum up, the the Mitosis marries the no-regret MAB algo-  
 240 rithms with the StemArm structure. We leverage a faster  
 241 but noisy oracle Oracle<sub>small</sub> and use a no-regret MAB algo-  
 242 rithm to guide the explore. The combinatorial explosion in  
 243 the number of arms is addressed by grouping less-promising  
 244 arms into StemArm.

## 245 4 Experiments

246 We evaluate our proposed policies on two types of data: syn-  
 247 thetic and real. In the following sections, we describe the ex-  
 248 perimental setup and report results separately for each case.

### 249 4.1 Experiments on Synthetic Data

250 **Setup** We formulate the food rescue volunteer notification  
 251 problem as an instance of the Contextual Budget Bandit. In  
 252 this setting, there are  $K$  regions (food-donation sources) and  
 253  $N$  volunteers who can be notified to pick up a donation. Fig-  
 254 ure 1 Provides an illustrative example. At each epoch  $t \leq T$ ,  
 255 a trip arises from some region  $k \in [K]$ , and the decision is to  
 256 notify a set of volunteers via actions  $a_i^t$ , taking into account  
 257 their current states  $s_i^t$  and the region context.

258 The states of volunteers are governed by the following tran-  
 259 sition dynamics:

- 260 • Only active volunteers ( $s_i = 1$ ) can pick up tasks  
 261 ( $r_i(0, a_i; k) = 0$  for all  $i, a_i, k$ ).
- 262 • A notified volunteer ( $a_i = 1$ ) is more likely to pick up a  
 263 task, i.e.,  $r_i(1, 1; k) \geq r_i(1, 0; k)$  for all  $i, k$ .
- A notified volunteer is more likely to become inactive:

$$P_i[s_i^{t+1} = 0 \mid s_i, a_i = 1] \geq P_i[s_i^{t+1} = 0 \mid s_i, a_i = 0].$$

264 The decision maker’s reward is defined as the total expected  
 265 pick-up rate over all volunteers.

266 **Volunteer Activity** We describe the construction of two  
 267 synthetic setups that capture different volunteer dynamics in  
 268 the food rescue problem (details in Appendix D.1)

---

### Algorithm 1 Mitosis

---

**Input:** Feasible region  $\mathcal{B}_0$ , LP upper-bound function LP, fast  
 oracle Oracle<sub>small</sub>

**Auxiliary:** UCB-type no-regret algorithm  $I_t(\cdot)$

**Output:** Budget allocation  $\vec{B}^*$  with high empirical re-  
 ward

1: **Initialize:**

- Initialize StemArm :=  $\{\mathcal{B}_0\}$ .
- Candidate set (heap)  $\mathcal{A} \leftarrow \{\text{StemArm}\}$ .
- Set time  $t \leftarrow 0$ .

2: **while**  $t < T$  **and** stopping condition not met **do**

3: Select from candidate set w.r.t. UCB index:

$$a^* \leftarrow \arg \max_{a \in \mathcal{A}} I_t(a),$$

4: **if**  $a^*$  is a **standard arm** (i.e., corresponds to a specific  
 $\vec{B}$ ) **then**

5: Pull arm and observe reward  $r_t(a^*) \leftarrow$   
 Oracle<sub>small</sub>( $\vec{B}$ ).

6: Update the empirical statistics  $N_t(a^*)$  and  $\hat{\mu}_t(a^*)$ .

7: **else**

8: //  $a^*$  is a **StemArm**; **splits out and pull new arm.**  
 9: StemArm splits arm  $a^*$  to obtain a new standard arm  
 $a'$  with allocation  $\vec{B}_{a'} = \vec{B}_{\text{new}}$ .

10: **Pull** new arm  $a'$ .

11: **Insert**  $a'$  into the candidate set:  $\mathcal{A} \leftarrow \mathcal{A} \cup \{a'\}$ .

12: **end if**

13:  $t \leftarrow t + 1$ , update the candidate set  $\mathcal{A}$  with  $I_{t+1}(\cdot)$ .

14: **end while**

15: **return** The allocation  $\vec{B}^*$  corresponding to the arm in  $\mathcal{A}$   
 with the highest empirical mean reward.

---

• **High Activeness** The  $N$  volunteers and  $K$  regions 269  
 are randomly distributed over a two-dimensional plane. 270  
 Each volunteer’s decision to pick up a task is influenced 271  
 by factors such as region popularity, distance, and per- 272  
 sonal engagement history. 273

• **Low Activeness** We introduce more challenging condi- 274  
 tions. by partitioning the  $K$  a subset of *nasty* regions and 275  
 its complement. In nasty regions, volunteers experience 276  
 high pick-up rates that tend to deactivate them quickly, 277  
 whereas in the remaining regions the rates are signifi- 278  
 cantly lower. 279

**The Effect of Volunteer Abundance and Budget on** 280  
**COcc’s Performance** Activity reflects the scarcity of vol- 281  
 unteer resources. We can systematically vary the abundance 282  
 of volunteers by tuning an *abundance ratio*  $\rho_{\text{Abundance}} \in [0, 1]$ : 283  
 $\rho_{\text{Abundance}}$  of the  $N$  volunteers follow the High Activeness dy- 284  
 namics, while the remainder operate under the Low Active- 285  
 ness dynamics. 286

We systematically vary Abundance  $\rho_{\text{Abundance}}$  and budget  $B$  287  
 to compare the performance between COcc against the opti- 288  
 mal Mitosis Algorithm, and plot the heatmap of COcc’s per- 289  
 formance in Figure 2. When the volunteer resource is scarce 290

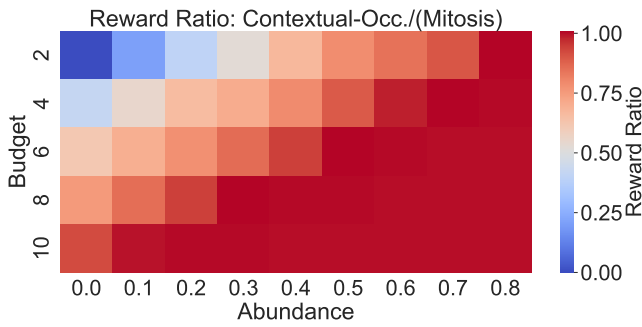


Figure 2: Reward ratio of COcc vs. Mitosis for [20] arms and [3] contexts across 32 seeds, varying Budget (vertical) and Abundance Ratio (horizontal). Red indicates near-optimal performance; blue indicates underperformance.

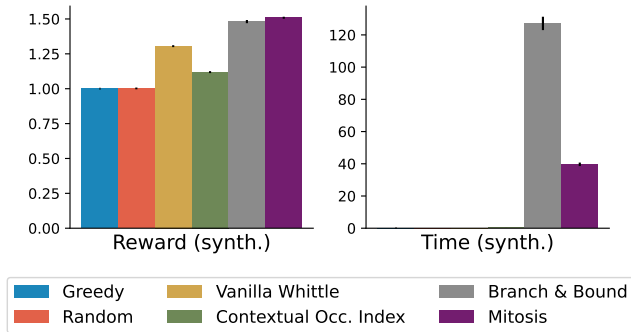


Figure 3: Main synthetic experiment with 50 arms, 3 contexts, 0.1 budget proportion, and 50% abundance. Bars show mean reward (left) and runtime (right) over 32 seeds. Mitosis yields the highest reward at significantly lower computation than Branch And Bound.

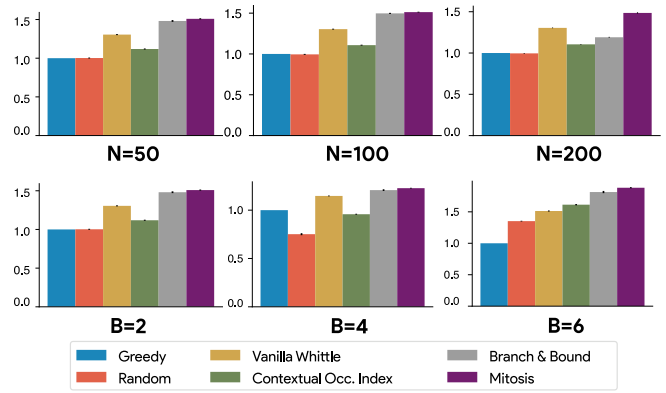


Figure 4: Ablations on Synthetic Data: Changing # Volunteers (First Row) and # budget (Second Row).

100, 200), the number of regions ( $K = 5, 10$ ) and budgets (315  
 $B = 2, 10$ ) respectively. Figure 4 shows the rewards of 316  
the various algorithms when varying  $N$  and  $B$ . Due to page 317  
limit, we defer the time plots and other reward plots to Ap- 318  
pendix D.2. The Mitosis and Branch And Bound policies 319  
consistently perform best. COcc’s performance, as the scale 320  
of the problem increases in either  $N, K, B$ , catches up with 321  
optimal, indicating that COcc performs generally better in 322  
larger scale problems. 323

Overall, in synthetic food rescue CBB problem, Mitosis 324  
provides optimal reward comparative to Branch And Bound 325  
with modest runtime. COcc—though much faster—does not 326  
fully match Mitosis’s optimal performance, and catches up as 327  
the problem scales up. 328

## 4.2 Experiments on Real Data 329

The experimental framework for real data mirrors that of 330  
the synthetic instance. The key difference is that the vol- 331  
unteers’ and regions’ attributes (historical engagement, loca- 332  
tion, and other idiosyncratic factors) are obtained from 333  
real-world datasets. We sample from a total pool of more than 500 334  
thousand volunteers to construct the CBB instance. The state 335  
transitions and reward definitions remain identical to those 336  
described for synthetic data, ensuring that the same policies 337  
can be fairly compared across both domains. 338

We evaluate the same set of policies as in the synthetic ex- 339  
periments: COcc, Mitosis, Random, Greedy, Vanilla Whittle, 340  
and Branch And Bound. The main experiment on a Real In- 341  
stance is run using 32 seeds with 100 trials per seed (Figure 5 342  
and performance is measured in terms of the normalized re- 343  
ward (total accumulated reward divided by that of the random 344  
policy). 345

On real data, the context-aware methods (COcc, Branch 346  
And Bound and Mitosis) outperform Greedy, Random and 347  
Vanilla Whittle. Branch And Bound yields the highest aver- 348  
age reward but requires disproportionately longer runtimes. 349  
By contrast, Mitosis nearly matches Branch And Bound while 350  
significantly reducing computation. Notably, COcc catches 351  
up with Mitosis—confirming it benefits from real-world at- 352  
tribute structure. The policies’ performance trend is sim- 353

291 (low  $\rho_{\text{Abundance}}$ ) or the notification budget  $B$  is small, COcc 292  
tends to lag behind compared to Mitosis (see top-left blue 293  
cells of Figure 2, where the reward ratio is almost close to 0). 294  
Low budget and low  $\rho_{\text{Abundance}}$  show joint degrade effect for 295  
COcc.

296 **Main Experiment** For food rescue problem formulated as 297  
CBB using synthetic data, we compare our proposed policies 298  
(CBB and Mitosis) with several benchmarks: *Random* policy 299  
that selects arms uniformly at random; *Greedy* policy that 300  
selects arms with the highest immediate reward  $r_i(s_i^t, 1, k)$ , the 301  
aforementioned Vanilla Whittle policy from standard RMAB, 302  
and Branch And Bound. We report cumulative reward nor- 303  
malized by Random and runtime, measured in seconds.

304 In a representative synthetic instance (50 arms, 3 contexts, 305  
budget= 5, 50% abundance), we run main experiments for 306  
the six aforementioned policies across 32 seeds (100 trials 307  
each). As shown in Figure 3 Mitosis (purple) achieves the 308  
highest reward overall, while Branch And Bound (gray) is 309  
also strong but much slower. The simpler baselines (Greedy, 310  
Random, Vanilla Whittle, and COcc), though taking almost 311  
no time to run, provide moderate to lower rewards, with the 312  
COcc notably underperforming at this abundance level.

313 **Ablation Studies on synthetic data** are conducted us- 314  
ing 32 seeds by varying the number of volunteers ( $N =$

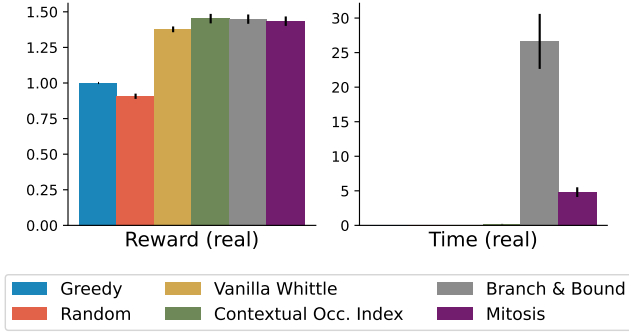


Figure 5: Experiment on real data. Bars show mean reward (left) and runtime (right) across 32 seeds (hatched to distinct real food rescue data). COcc, Branch And Bound and Mitosis perform equally well. Branch And Bound takes significantly more time to reach optimal.

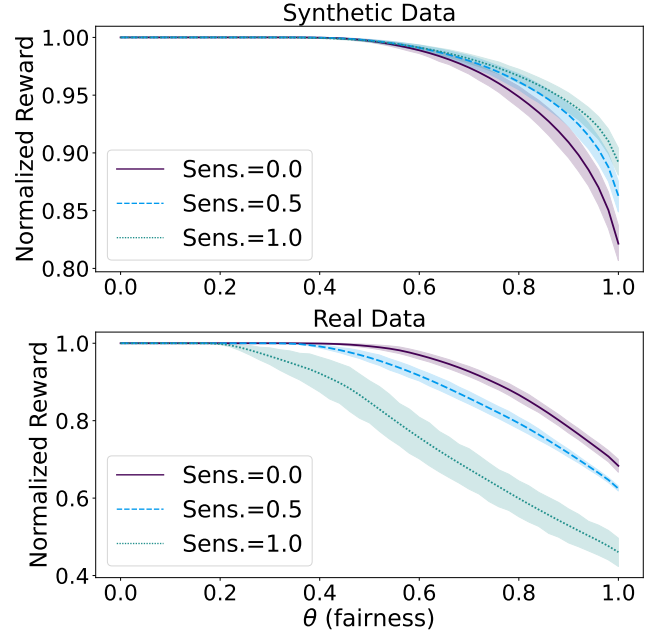


Figure 6: Pareto frontiers ( $\theta$  vs. reward). Volunteer distance-sensitivity is shown in different line style. Heightened sensitivity makes fair solutions more costly in terms of total reward in real data.

ilar when we vary the number of volunteers, the number of regions and budget level in the ablation studies (see Appendix D.2 for details). This implies in application, COcc is sufficient for near-optimal performance. Mitosis guarantees optimality and is significantly faster than Branch And Bound.

## 5 Case Study: Fairness in Food Rescue

**Geographical disparity in Food Rescue** Food rescue organizations potentially suffer from geographic disparity where harder-to-reach areas are ignored. Over time, this can turn into a form of algorithmic discrimination, where certain regions or demographics are consistently underserved. We build on prior work that analyzes proportional fairness in RMABs [Li and Varakantham, 2022a; Wang *et al.*, 2024; Li and Varakantham, 2022b; Killian *et al.*, 2023] and develop a natural proportional fairness definition to enforce fairness across contexts in CBB. **The intuition is that a region’s reward should be at least a fraction  $\theta$  of the total reward multiplied by the region’s occurrence probability.**

**Definition 5.1 ( $\theta$ -Fair).** For a contextual-RMAB instance, a budget allocation  $\vec{B}$  is  $\theta$ -Fair if the reward for each context divided by the occurrence probability of the context, is at least a fraction  $\theta$  of its scaled share of the total reward in the solution of occupancy-measure LP (1):

$$\theta \left( \underbrace{\sum_i \sum_k \sum_{s_i, a_i} \mu_i(s_i, a_i; k) r_i(s_i, a_i; k)}_{\text{total reward}} \right) \quad (13)$$

$$\leq \underbrace{\frac{1}{f_k} \sum_i \sum_{s_i, a_i} \mu_i(s_i, a_i; k) r_i(s_i, a_i; k)}_{\text{reward for type } k}, \quad \forall k. \quad (14)$$

$\theta$  ranges on  $[0, 1]$  and it tunes the fairness level. When  $\theta = 0$  no fairness is imposed, while  $\theta = 1$  enforces full fairness. For a fixed  $\theta$ , the  $\theta$ -Fair definition is linear in  $\mu(\cdot, \cdot; \cdot)$ . Hence, we can incorporate it into occupancy-measure LP and solve for a budget allocation  $\vec{B}$  satisfying the  $\theta$ -constraint, using estimates from the COcc.

**Insights from Real Data Experiment** We study how increasing fairness constraints ( $\theta \in [0, 1]$ ) affect total reward, plotting this trade-off as a Pareto frontier in Figure 6 for both synthetic (left) and real (right) instances. A critical parameter in our model is volunteers’ *sensitivity to distance*, which reduces pick-up rates for more remote locations. When sensitivity increases, it becomes harder to serve distant or underserved areas. As the fairness parameter  $\theta$  grows under higher distance sensitivity, total reward declines more sharply.

## 6 Related Works

**Restless Multi-Armed Bandits** is a model of decision-making which extends multi-armed bandits so each arm has a state. While finding optimal actions for an RMAB is an NP-hard problem [Papadimitriou and Tsitsiklis, 1994], early work in the RMAB space proposed the Whittle index policy [Whittle, 1988] and demonstrated the asymptotic optimality of such a policy [Weber and Weiss, 1990a]. RMABs have seen increased attention recently due to its applicability for a range of real-world problems from maternal health [Mate *et al.*, 2022] to food rescue [Raman *et al.*, 2024] to autonomous vehicles [Li *et al.*, 2021]. Within contextual RMABs, lines of work include Bayesian transitions [Liang *et al.*, 2024], global contexts for demand modeling [Chen *et al.*, 2024], and using neural networks to predict indices [Guo and Wang, 2024]. Our work can be seen as an intersection between the application and technical lines of work, as we extend RMABs to varying budget contextual settings and apply these ideas to the food rescue domain.

**Food Rescue** are volunteer-driven organizations focusing on redistributing food Shi *et al.* [2020]. Prior works fre-

413 quently utilize AI to model volunteer engagements [Man-  
414 shadi and Rodilitz, 2020; Raman *et al.*, 2024], predicted trip  
415 difficulties [Shi *et al.*, 2024], and developed a recommender  
416 system for matching volunteers [Shi *et al.*, 2021]. We build  
417 on the volunteer engagement literature and address the is-  
418 sue of geographic disparity reported by prior work Shi *et al.*  
419 [2021].

420 **Fairness** is an increasingly important consideration in both  
421 business and non-profit organizations Bertsimas *et al.* [2012];  
422 Liu and Garg [2024]. For RMAB, fairness is typically im-  
423 posed on individual arms: Wang *et al.* [2024] define fairness  
424 as requiring a minimum long-term activation fraction for each  
425 arm; Li and Varakantham [2022b] propose a *soft fairness con-*  
426 *straint*, or by setting an upperbound on the number of deci-  
427 sion epochs since an arm was last activated (Li and Varakan-  
428 tham [2022a]). Fairness can also be defined over groups of  
429 arms. Killian *et al.* [2023] study minimax and max-Nash  
430 welfare objectives by imposing fairness on groups of arms,  
431 and Verma *et al.* [2024] enforce fairness with respect to the  
432 reward outcomes across groups. To the best of our knowl-  
433 edge, although RMABs with **contextual information** have  
434 been previously studied, our work is the first to consider fair-  
435 ness with respect to **context**.



## 436 References

- 437 Peter Auer, Nicolò Cesa-Bianchi, and Paul Fischer. Finite-  
438 time analysis of the multiarmed bandit problem. *Mach.*  
439 *Learn.*, 47(2–3):235–256, May 2002.
- 440 Dimitris Bertsimas, Vivek F. Farias, and Nikolaos Trichakis.  
441 On the efficiency-fairness trade-off. *Management Science*,  
442 58(12):2234–2250, 2012.
- 443 Xin Chen, I Hou, et al. Contextual restless multi-armed band-  
444 its with application to demand response decision-making.  
445 *arXiv preprint arXiv:2403.15640*, 2024.
- 446 Alisha Coleman-Jensen, Matthew P Rabbitt, Christian A Gre-  
447 gory, and Anita Singh. Household food security in the  
448 united states in 2017. *USDA-ERS Economic Research Re-*  
449 *port*, 2018.
- 450 Zach Conrad, Meredith T Niles, Deborah A Neher, Eric D  
451 Roy, Nicole E Tichenor, and Lisa Jahns. Relationship be-  
452 tween food waste, diet quality, and environmental sustain-  
453 ability. *PLoS one*, 13(4):e0195405, 2018.
- 454 John Gittins, Kevin Glazebrook, and Richard Weber. *Restless*  
455 *Bandits and Lagrangian Relaxation*, chapter 6, pages 149–  
456 172. John Wiley & Sons, Ltd, 2011.
- 457 Zhanqiu Guo and Wayne Wang. Contextwin: Whittle index  
458 based mixture-of-experts neural model for restless bandits  
459 via deep rl. *arXiv preprint arXiv:2410.09781*, 2024.
- 460 Roch Guérin, Amy McGovern, and Klara Nahrstedt. Report  
461 on the nsf workshop on sustainable computing for sustain-  
462 ability (nsf wscs 2024), 2024.
- 463 Jackson A. Killian, Manish Jain, Yugang Jia, Jonathan Amar,  
464 Erich Huang, and Milind Tambe. Equitable restless multi-  
465 armed bandits: A general framework inspired by digital  
466 health, 2023.
- 467 Dexun. Li and Pradeep Varakantham. Efficient resource al-  
468 location with fairness constraints in restless multi-armed  
469 bandits. In James Cussens and Kun Zhang, editors, *Pro-*  
470 *ceedings of the Thirty-Eighth Conference on Uncertainty*  
471 *in Artificial Intelligence*, volume 180 of *Proceedings of*  
472 *Machine Learning Research*, pages 1158–1167. PMLR,  
473 01–05 Aug 2022.
- 474 Dexun Li and Pradeep Varakantham. Towards soft fairness in  
475 restless multi-armed bandits, 2022.
- 476 Mushu Li, Jie Gao, Lian Zhao, and Xuemin Shen. Adap-  
477 tive computing scheduling for edge-assisted autonomous  
478 driving. *IEEE Transactions on Vehicular Technology*,  
479 70(6):5318–5331, 2021.
- 480 Biyonka Liang, Lily Xu, Aparna Taneja, Milind Tambe, and  
481 Lucas Janson. A bayesian approach to online learning  
482 for contextual restless bandits with applications to public  
483 health. *arXiv preprint arXiv:2402.04933*, 2024.
- 484 Zhi Liu and Nikhil Garg. Redesigning service level agree-  
485 ments: Equity and efficiency in city government opera-  
486 tions. In *Proceedings of the 25th ACM Conference on Eco-*  
487 *nomics and Computation*, EC ’24, page 309, New York,  
488 NY, USA, 2024. Association for Computing Machinery.
- Vahideh Manshadi and Scott Rodilitz. Online policies  
for efficient volunteer crowdsourcing. *arXiv preprint*  
*arXiv:2002.08474*, 2020.
- Aditya Mate, Jackson Killian, Haifeng Xu, Andrew Perrault,  
and Milind Tambe. Collapsing bandits and their applica-  
tion to public health intervention. *Advances in Neural In-*  
*formation Processing Systems*, 33:15639–15650, 2020.
- Aditya Mate, Lovish Madaan, Aparna Taneja, Neha Mad-  
hiwalla, Shresth Verma, Gargi Singh, Aparna Hegde,  
Pradeep Varakantham, and Milind Tambe. Field study  
in deploying restless multi-armed bandits: Assisting non-  
profits in improving maternal and child health. In *Proce-*  
*edings of the AAAI Conference on Artificial Intelligence*, vol-  
ume 36-11, pages 12017–12025, 2022.
- Christos H Papadimitriou and John N Tsitsiklis. The com-  
plexity of optimal queueing network control. In *Proce-*  
*edings of IEEE 9th annual conference on structure in com-*  
*plexity Theory*, pages 318–322. IEEE, 1994.
- Justin Payan and Yair Zick. I will have order! optimiz-  
ing orders for fair reviewer assignment. *arXiv preprint*  
*arXiv:2108.02126*, 2021.
- Naveen Janaki Raman, Zheyuan Ryan Shi, and Fei Fang.  
Global rewards in restless multi-armed bandits. In *The*  
*Thirty-eighth Annual Conference on Neural Information*  
*Processing Systems*, 2024.
- Zheyuan Ryan Shi, Yiwen Yuan, Kimberly Lo, Leah  
Lizarondo, and Fei Fang. Improving efficiency of  
volunteer-based food rescue operations. *Proceedings of the*  
*AAAI Conference on Artificial Intelligence*, 34(8):13369–  
13375, 2020.
- Zheyuan Ryan Shi, Leah Lizarondo, and Fei Fang. A recom-  
mender system for crowdsourcing food rescue platforms.  
In *Proceedings of the Web Conference 2021*, pages 857–  
865, 2021.
- Zheyuan Ryan Shi, Jiayin Zhi, Siqi Zeng, Zhicheng Zhang,  
Ameesh Kapoor, Sean Hudson, Hong Shen, and Fei Fang.  
Predicting and presenting task difficulty for crowdsourcing  
food rescue platforms. In *Proceedings of the ACM on Web*  
*Conference 2024*, pages 4686–4696, 2024.
- Shresth Verma, Yunfan Zhao, Sanket Shah, Niclas Boehmer,  
Aparna Taneja, and Milind Tambe. Group fairness in  
predict-then-optimize settings for restless bandits. In Ne-  
gar Kiyavash and Joris M. Mooij, editors, *Proceedings of*  
*the Fortieth Conference on Uncertainty in Artificial Intel-*  
*ligence*, volume 244 of *Proceedings of Machine Learning*  
*Research*, pages 3448–3469. PMLR, 15–19 Jul 2024.
- Shufan Wang, Guojun Xiong, and Jian Li. Online restless  
multi-armed bandits with long-term fairness constraints.  
*Proceedings of the AAAI Conference on Artificial Intelli-*  
*gence*, 38(14):15616–15624, Mar. 2024.
- Richard R Weber and Gideon Weiss. On an index policy for  
restless bandits. *Journal of applied probability*, 27(3):637–  
648, 1990.

- 542 Richard R. Weber and Gideon Weiss. On an index pol-  
543 icy for restless bandits. *Journal of Applied Probability*,  
544 27(3):637–648, 1990.
- 545 Peter Whittle. Restless bandits: Activity allocation in  
546 a changing world. *Journal of applied probability*,  
547 25(A):287–298, 1988.
- 548 Guojun Xiong, Jian Li, and Rahul Singh. Reinforcement  
549 learning augmented asymptotically optimal index policy  
550 for finite-horizon restless bandits. *Proceedings of the AAAI*  
551 *Conference on Artificial Intelligence*, 36(8):8726–8734,  
552 Jun. 2022.

## 553 A Proof of Theorem 1

□ 586

**Theorem 1.** For a CBB, denote the Whittle Index Policy’s reward as  $\mathcal{R}^{\text{VanillaWhittle}}$ , and the optimal policy that satisfies context-specific budget constraint as  $\mathcal{R}^{\text{ContextOpt}}$ . There exists an instance where,

$$\frac{\mathcal{R}^{\text{ContextOpt}}}{\mathcal{R}^{\text{VanillaWhittle}}} \rightarrow \infty, \quad \text{as } N \rightarrow \infty.$$

554 *Proof.* Consider a CBB instance with  $N$  stochastically identical arms. For simplicity we assume that the transition probabilities are such that each arm is always active ( $s_i = 1$ ).  
555 Let there be two contexts, where context 1 occurs with probability  
556  $f_1 = 1 - \frac{1}{N}$  and context 2 occurs with probability  
557  $f_2 = \frac{1}{N}$ . For each arm  $i$ , context 1 generates reward  
558  $r_i(s_i = 1, a_i = 1) = \frac{1}{N}$ , context 2 generates reward  
559  $r_i(s_i = 1, a_i = 1) = N$ . Suppose budget  $B = 1$ .

560 Consider the policy that leaves all arms idle at context 1,  
561 and pulls all  $N$  arms at context 2. The policy is feasible be-  
562 cause its budget constraint  $\vec{B} = (0, N)$  satisfies  $f_1 \times 0 + f_2 \times$   
563  $N = \frac{1}{N} \times N = 1 = B$ . Its average reward is  $N$ .

564 For Vanilla Whittle Index Policy, the good context 2 that  
565 has the high reward only occurs with probability  $\frac{1}{N}$ . And  
566 when it happens, we can only pull and get reward from *one*  
567 arm. So its average reward is  $(1 - \frac{1}{N})\frac{1}{N} + \frac{1}{N} \times N = O(1)$ .  
568 As  $N \rightarrow \infty$ , the gap between the two policies goes to infin-  
569 ity. □

## 572 B Dual of the occupancy-measure LP

573 *Proof.* Let  $V_i(s_i, k), \forall i, s_i, k$  be the Lagrangian for con-  
574 straint (2, 3). Let  $\nu_i, \forall i$  be the Lagrangian multiplier for (4),  
575 and  $\rho$  for (5). The dual of the occupancy-measure LP (1) is

$$\min_{V_i, \rho, \nu} \sum_{i \in [M]} \nu_i + \rho B \quad (15)$$

$$\text{s.t. } V_i(s_i, k) + \nu_i \geq r_i(s_i, a_i; k) - \rho \mathbb{I}\{a_i = 1\} \quad (16)$$

$$+ \sum_{s'_i, k'} V_i(s'_i, k') P[s_i \rightarrow s'_i | a_i, k], \forall s_i, a_i, k \quad (17)$$

$$\rho \geq 0 \quad (18)$$

576 Then it is to show that for every  $(s_i, k)$  combination, at  
577 least one inequality in (16) is tight. By complementary slack-  
578 ness, a pair of optimal primal-dual variables  $(\mu^*, V^*, \nu^*, \rho^*)$   
579 would satisfy  $\mu_i^*(s_i, a_i; k) > 0$  only if constraint (16) is tight.  
580 (Assume non-degeneracy that every state-action  $s_i, k$  is of  
581 positive occupancy measure) for any arm  $i$  and state-context  
582 pair  $(s_i, k)$ , at least one action  $a_i$  needs to be chosen, i.e.  
583  $\exists a_i, \mu_i^*(s_i, a_i, k) > 0$ , which implies that

$$\begin{aligned} V_i^*(s_i, k) + \nu_i^* &= r_i(s_i, a_i; k) - \rho^* \mathbb{I}\{a_i = 1\} \\ &+ \sum_{s'_i, k'} V_i^*(s'_i, k') P[s_i \rightarrow s'_i | a_i, k]. \end{aligned}$$

584 Combined with the rest of  $a_i \in \mathcal{A}$  and inequalities in 16,  
585 we have

$$\begin{aligned} V_i^*(s_i, k) + \nu_i^* &= \max_{a_i \in \{0,1\}} (r_i(s_i, a_i; k) - \rho^* \mathbb{I}\{a_i = 1\}) \\ &+ \sum_{s'_i, k'} V_i^*(s'_i, k') P[s_i \rightarrow s'_i | a_i, k]. \end{aligned}$$

## 587 C Proof of Theorem 2

**Theorem 2.** The COcc’s asymptotic approximation ratio  
588 compared to  $\mathcal{R}^{\text{ContextOpt}}$  is bounded above by  $\frac{5}{6}$ .  
589

*Proof. Outline* First, we formally establish the asymptotic  
590 framework, which is where the Whittle Index Policy for stan-  
591 dard RMAB achieves optimality. Then we introduce how to  
592 analyze CBB’s in this asymptotic regime. Finally, we present  
593 the instance where the  $\frac{5}{6}$  bound is achieved.  
594

### 595 Asymptotic Notion

We define the asymptotic notion for analyzing (sub-  
596)optimality for CBB. It is same to the approach for standard  
597 RMAB, originally proposed by Weber and Weiss [1990b] for  
598 RMAB with stochastically identical arms and generalized to  
599 heterogeneous arms by Xiong *et al.* [2022]:  
600

**Definition C.1** ( $\rho$ -scaled CBB). Fix a *Base* CBB instance  
with  $M$  arms

$$\langle M, \mathcal{S}, \mathcal{A}, K, \{r_i^k\}_{i \in [M], k \in \mathcal{K}}, \{P_i^k\}_{i \in [M], k \in \mathcal{K}}, \mathcal{F} \rangle.$$

With budget  $B \in \mathbb{N}$ .

Now, consider each arm being replicated  $\rho$  times, with the  
602 budget scaled by  $\rho$  as well. The new CBB instance has  $\rho \times M$   
603 arms, with each of the  $M$  arms in the base CBB repeated  $\rho$   
604 times. Budget is scaled to  $\rho B$ .  
605

For a base contextual RMAB instance scaled with  $\rho$ , when  
606 there is no confusion about the base instance we’re referring  
607 to, denote its reward for any policy  $\pi$  as

$$\mathcal{R}^\pi(\rho) := \lim_{T \rightarrow \infty} \mathbb{E}_{\vec{a} \sim \pi(\cdot), k \sim \mathcal{F}} \left[ \frac{1}{T} \sum_{t=1}^T \sum_{i \in [\rho M]} r_i^k(s_i^t, a_i^t) \right].$$

For  $\rho$ -scaled CBB, notice that its reward upperbound from  
608 solving the occupancy-measure LP (1) simply scales with  $\rho$ :

$$\overline{\mathcal{R}}(\rho) = \rho \overline{\mathcal{R}}(1).$$

We refer to every arm  $i \in [M]$  in the base instance as a  
606 **type- $i$**  arm, and its  $\rho$  replicates in the  $\rho$ -scaled CBB as the  $\rho$   
607 type- $i$  arms.  
608

### 609 Asymptotic System Behavior for CBB

In the following section we introduce a new method for ana-  
610 lyzing the asymptotic behavior of CBB as  $\rho \rightarrow \infty$ . It is differ-  
611 ent from the standard approach of Weber and Weiss [1990b].  
612

To ease the complication of notations, we describe our  
613 method with CBB that  $r_i(s_i = 0, a = 0; k) = r_i(s_i =$   
614  $0, a = 1; k) = 0, \forall i, k$ , and transition probabilities  $P_i^k s_i^{t+1} |$   
615  $s_i^t, a_i^t = 1] = P_i^k s_i^{t+1} | s_i^t, a_i^t = 0], \forall s_i^{t+1}, s_i^t$ . In this way it  
616 is meaningless to pull inactive arms, since it makes no differ-  
617 ence in rewards nor transition probabilities. Generalization to  
618 general CBB is without loss of generality.  
619

We care about the proportion of active arms as  $\rho \rightarrow \infty$   
620 of the  $\rho$ . The following technical lemma characterizes the  
621 dynamic of arms:  
622

623 **Lemma 1.** Denote as  $a_i^t$  the proportion of type- $i$  active arms  
624 at any time point  $t$  under given policy  $\pi$ . Conditional on  $a_i^t$   
625 and context  $k$ ,  $a_i^{t+1}$ 's distribution converges to a Direc Delta  
626 function  $\delta_{\text{shift}}(\cdot)$ , shifted with  $\mathbb{E}[a_i^{t+1} | a_i^t, k]$  as the total num-  
627 ber of arms  $\rho \rightarrow \infty$ . In other words,

$$f(a_i^{t+1} | a_i^t, k) = \delta_{\mathbb{E}[a_i^{t+1} | a_i^t, k]}(a_i^{t+1}), \quad (19)$$

628 where, let  $B_{i,k}$  be the number of active type- $i$  arms pulled by  
629 the policy at context  $k$ :

$$\mathbb{E}[a_i^{t+1} | a_i^t, k] = \min(a_i^t, \frac{B_{i,k}}{\rho}) P_i^k s_i^{t+1} = 1 | s_i^t = 1, a_i^t = 1] \quad (20)$$

$$+ (a_i^t - \min(a_i^t, \frac{B_{i,k}}{\rho}) \quad (21)$$

$$\times P_i^k s_i^{t+1} = 0 | s_i^t = 1, a_i^t = 1] \quad (22)$$

$$+ (1 - a_i^t) P_i^k s_i^{t+1} = 1 | s_i^t = 0] \quad (23)$$

630 *Proof.* The sketch of the proof is that, the **number** of active  
631 arms is sum of Binomial random variables, with parameters  
632 given by the policy and transition probabilities. As total  
633 number of arms  $\rho \rightarrow \infty$ , each Binomial variable divided by  $\rho$   
634 converges to (shifted) Direc Delta. Therefore, the *proportion*  
635 of active arms is also (shifted) Direc Delta.

636 **Notes on Binomial Distribution** To make later analysis  
637 clear, first consider a single binomial random variable  $X$  with  
638  $N$  experiments and success rate  $p$  (i.e.  $X \sim \text{Bin}(N, p)$ ). For  
639 any  $x \in [0, 1]$  (assume  $Nx$  is integer):

$$P[X = Nx] = \binom{N}{Nx} p^{Nx} (1-p)^{N(1-x)}$$

$$\text{Apply Stirling's Formula: } n! \sim \sqrt{2\pi n} \cdot \left(\frac{n}{e}\right)^n$$

$$= \sqrt{\frac{1}{x(1-x)N}} \cdot \left(\left(\frac{p}{x}\right)^x \left(\frac{1-p}{1-x}\right)^{(1-x)}\right)^N$$

It can be verified that  $\left(\frac{p}{x}\right)^x \left(\frac{1-p}{1-x}\right)^{(1-x)} < 1$  for  $x \neq p$ . There-  
fore, as  $N \rightarrow \infty$

$$P[X = xN] = \begin{cases} \sqrt{\frac{1}{x(1-x)N}} \rightarrow \infty & x = p \\ \sqrt{\frac{1}{x(1-x)N}} \times \mathcal{O}\left(\left(\left(\frac{p}{x}\right)^x \left(\frac{1-p}{1-x}\right)^{(1-x)}\right)^N\right) \rightarrow 0 & x \neq p \end{cases}$$

640 Therefore, say if we let  $f(x) = P[X = xN]$ ,  $f(\cdot)$  is a  
641 shifted-to- $p$  Direc Delta function.

642 **Stationary Distribution Contextual Budget Bandit** Let  
643  $A_i^t := a_i^t \rho$  denote the **number of active type- $i$  arms** at time  
644 point  $t$ . Conditional on current  $A_i^t$  and context  $k$ ,

645 •  $\min(A_i^t, B_{i,k})$  arms are pulled, where each arm remains  
646 active w.p.  $P_i^k s_i^{t+1} = 1 | s_i^t = 1, a_i^t = 1]$ .

647 • Each of  $\rho - A_i^t$  inactive arms transfers back to active w.p.  
648  $P_i^k s_i^{t+1} = 1 | s_i^t = 0]$ ,

Therefore, the number of active arms at next period  $A_i^{t+1}$  is 649  
the sum of three binomial random variables: 650

$$\{A_i^{t+1} | A_i^t, k\} \quad (24)$$

$$\sim \underbrace{\text{Bin}(\min\{A_i^t, B_{i,k}\}, P_i^k s_i^{t+1} = 1 | s_i^t = 1, a_i^t = 1)}_{\text{active arms pulled staying active}} \quad (25)$$

$$+ \underbrace{\text{Bin}(A_i^t - \min\{A_i^t, B_{i,k}\}, P_i^k s_i^{t+1} = 1 | s_i^t = 1, a_i^t = 0)}_{\text{idle active arms staying active}} \quad (26)$$

$$+ \underbrace{\text{Bin}(\rho - A_i^t, P_i^k s_i^{t+1} = 1 | s_i^t = 0)}_{\text{inactive arms transfer back to active}}. \quad (27)$$

Scaled by  $\rho \rightarrow \infty$ , each of the above binomial distribu- 651  
tion converges to a Direc Delta function centered on its 652  
mean. Since adding up random variables is equivalent to tak- 653  
ing convolution of their probability mass functions—Direc 654  
Delta functions are closed under convolution—random vari- 655  
able  $a_i^{t+1} = \frac{A_i^{t+1}}{\rho}$ 's probability mass function is a Direc Delta 656  
shifted by  $\frac{1}{\rho} \mathbb{E}[A_i^{t+1} | A_i^t, k]$ .  $\square$  657

The lemma implies, the *proportion* of active arms  $a_i^t$  evolve 658  
“almost deterministically”—more precisely speaking, fix any 659  
policy  $\pi$ , if at current time step the proportion of active arms 660  
is  $a_i^t$ , context is  $k$ , the next time step will have  $(\mathbb{E}[a_i^{t+1} |$  661  
 $a_i^t, k])\%$  active arms almost surely, where  $(\mathbb{E}[a_i^{t+1} | a_i^t, k])$  is 662  
given by the following: 663

$$\begin{aligned} & \mathbb{E}[a_i^{t+1} | a_i^t, k] \\ &= \frac{1}{\rho} \mathbb{E}[A_i^{t+1} | A_i^t, k] \\ &= \frac{1}{\rho} \mathbb{E}[\underbrace{\text{Bin}(\min\{A_i^t, B_{i,k}\}, P_i^k s_i^{t+1} = 1 | s_i^t = 1, a_i^t = 1)}_{\text{active arms pulled}} \\ & \quad + \underbrace{\text{Bin}(A_i^t - \min\{A_i^t, B_{i,k}\}, P_i^k s_i^{t+1} = 1 | s_i^t = 1, a_i^t = 0)}_{\text{untouched active arms}} \\ & \quad + \underbrace{\text{Bin}(\rho - A_i^t, q_i)}_{\text{inactive arms}}] \\ &= \frac{1}{\rho} (\min\{A_i^t, B_{i,k}\} \cdot P_i^k s_i^{t+1} = 1 | s_i^t = 1, a_i^t = 1] \\ & \quad + (A_i^t - \min\{A_i^t, B_{i,k}\}) \cdot P_i^k s_i^{t+1} = 1 | s_i^t = 1, a_i^t = 0] \\ & \quad + (\rho - A_i^t) q_i \end{aligned}$$

Denote  $\beta_{i,k} := \frac{B_{i,k}}{\rho}$ : 664

$$\mathbb{E}[a_i^{t+1} | a_i^t, k] \quad (28)$$

$$= \min(a_i^t, \beta_{i,k}) \cdot P_i^k s_i^{t+1} = 1 | s_i^t = 1, a_i^t = 1] \quad (29)$$

$$+ \max(a_i^t - \beta_{i,k}, 0) \cdot P_i^k s_i^{t+1} = 1 | s_i^t = 1, a_i^t = 0] \quad (30)$$

$$+ (1 - a_i^t) P_i^k s_i^{t+1} = 1 | s_i^t = 0] \quad (31)$$

If, current time step's proportion of active arms is  $x \in$  665  
 $[0, 1]$ , with probability  $f_k$  context  $k$  occurs, then the next time 666

667 step's active-arm proportion will be  $y = \mathbb{E}[a_i^{t+1} \mid x, k]$  (as  
668 given in 29-31) w.p.  $f_k$ . And for each  $y$ , define its inverse

$$\mathcal{X}(y) := \{(x, k) : \mathbb{E}[a_i^{t+1} \mid x, k] = y\}. \quad (32)$$

669 Denote the stationary distribution of proportion of active arms  
670 as  $\pi : [0, 1] \rightarrow [0, 1]$ , it should satisfy:

$$\pi(y) = \sum_{(x,k) \in \mathcal{X}(y)} f_k \pi(x). \quad (33)$$

### 671 C.1 A 5/6 Approximation Upperbound.

672 **An adversarial instance** Consider a base CBB example  
673 with only one type of arm (i.e.,  $M = 1$ ). Let there be  $\rho$   
674 copies of this arm in the scaled setting as  $\rho \rightarrow \infty$ . We drop  
675 the index  $i$  for convenience. Suppose there are two contexts,  
676  $k \in \{1, 2\}$ , each occurring with probability  $f_1 = f_2 = 0.5$ .

677 Let  $\epsilon > 0$ . The transition probabilities and rewards are  
678 defined as follows.

679 • Context 1: transition probabilities is

$$\begin{aligned} P^1[s^{t+1} = 1 \mid s = 1, a = 1] &= 1 - \epsilon \\ P^1[s^{t+1} = 0 \mid s = 1, a = 1] &= \epsilon \\ P^1[s^{t+1} = 1 \mid s = 1, a = 0] &= 1 \\ P^1[s^{t+1} = 0 \mid s = 1, a = 0] &= 0 \\ P^1[s^{t+1} = 1 \mid s = 1, \forall a = 0, 1] &= 1 \\ P^1[s^{t+1} = 0 \mid s = 1, \forall a = 0, 1] &= 0 \end{aligned}$$

680 reward for context 1:

$$\begin{aligned} r(s^t = 1, a^t = 1; k = 1) &= 1 \\ r(s^t = 1, a^t = 0; k = 1) &= 0 \\ r(s^t = 0, a^t = 1; k = 1) &= 0 \\ r(s^t = 1, a^t = 0; k = 1) &= 0 \end{aligned}$$

681 • Context 2: transition probabilities is

$$\begin{aligned} P^2[s^{t+1} = 1 \mid s = 1, a = 1] &= 0 \\ P^2[s^{t+1} = 0 \mid s = 1, a = 1] &= 1 \\ P^2[s^{t+1} = 1 \mid s = 1, a = 0] &= 1 \\ P^2[s^{t+1} = 0 \mid s = 1, a = 0] &= 0 \\ P^2[s^{t+1} = 1 \mid s = 1, \forall a = 0, 1] &= 1 \\ P^2[s^{t+1} = 0 \mid s = 1, \forall a = 0, 1] &= 0 \end{aligned}$$

682 reward for context 2:

$$\begin{aligned} r(s^t = 1, a^t = 1; k = 1) &= 1 + \epsilon \\ r(s^t = 1, a^t = 0; k = 1) &= 0 \\ r(s^t = 0, a^t = 1; k = 1) &= 0 \\ r(s^t = 1, a^t = 0; k = 1) &= 0 \end{aligned}$$

683 **Budget** Assume that budget is  $1/3$  of the number of total  
684 arms. I.e. in the  $\rho$ -scaled instance,  $B = \lfloor \frac{1}{3} \rfloor$ . As the scaling  
685 factor  $\rho \rightarrow \infty$ , we can without loss of generality assume that  
686 it's an interger.

**The Reward for COcc** The occupancy-measure LP for the  
base instance simplifies to

$$\max_{\mu, B_k} \mu(1, 1, 1) + \mu(1, 1, 2)(1 + \epsilon)$$

subject to

$$\begin{aligned} (1 - P[s = 1]) &= \epsilon \mu(1, 1, 1) + \mu(1, 1, 2) \\ \mu(1, 1, k) &\leq \frac{1}{2} P[s = 1], \forall k = 1, 2 \\ \mu(1, 1, 1) + \mu(1, 1, 2) &\leq \frac{1}{3} \end{aligned}$$

The COcc then allocate budget following the optimal solu-  
tion ( $\mu^*$ ) of the occupancy-measure LP. For the  $\rho$ -scaled CBB  
with total budget  $B = \frac{1}{3}\rho$ , the budget allocation of COcc is

$$\begin{aligned} B_1 &= \rho \times \frac{1}{f_1} \mu^*(1, 1, 1) = 0, \\ B_2 &= \rho \times \frac{1}{f_2} \mu^*(1, 1, 2) = \frac{2}{3}. \end{aligned}$$

From (29-31) we obtain, as  $\rho \rightarrow \infty$ , the transition dynamic  
of the proportion of active arms  $x^t \rightarrow x^{t+1}$  in RMAB:

• With probability  $f_1 = 0.5$ , context  $k = 1$ :

$$x^{t+1} = \mathbb{E}[a_i^{t+1} \mid x^t, k] = 1;$$

• With probability  $f_2 = 0.5$ , context  $k = 2$ :

$$x^{t+1} = \mathbb{E}[a_i^{t+1} \mid x^t, k] = \max(x^t - \frac{2}{3}, 0) + 1 - x^t.$$

From 32 and 33 we obtain the stationary distribution  $\pi$  under  
Policy\* (actually, guess-and-verify)

$$\begin{aligned} \pi(\frac{1}{3}) &= \frac{1}{3}, \\ \pi(\frac{2}{3}) &= \frac{1}{6} \\ \pi(1) &= \frac{1}{2}, \\ \pi(x) &= 0, \text{ otw.} \end{aligned}$$

When the proportion of active arms =  $\frac{1}{3}$ —only half of the  
budget is utilized. This happens, as give above, w.p.  $\pi(\frac{1}{3}) =$   
 $\frac{1}{3}$ . So the reward as  $\rho \rightarrow \infty$  is

$$\begin{aligned} \mathcal{R}^{\text{COcc}}(\rho) &= f_2 \left( \frac{1}{3} \rho \pi(\frac{1}{3}) + \frac{2}{3} \rho \left( \pi(\frac{2}{3}) + \pi(1) \right) \right) \\ &= 0.5 \rho \left( \frac{1}{9} + \frac{4}{9} \right) = \frac{5}{18} \rho \end{aligned}$$

**Optimal Budget Allocation** However, notice that the other  
context  $k = 1$  is almost always active (it has probability  $p = \epsilon$   
of transfer to inactive). Therefore, if we allocate all budget to  
context 1:

$$B_1 = \frac{2}{3}, B_2 = 0$$

• The stationary reward for the optimal budget allocation is

$$\mathcal{R}^{\text{ContextOpt}}(\rho) = \frac{1}{3} \rho$$

Therefore, the COcc's approximation is bounded above by  $\frac{5}{6}$ .

$$\lim_{\rho \rightarrow \infty} \frac{\mathcal{R}^{\text{COcc}}(\rho)}{\mathcal{R}^{\text{ContextOpt}}(\rho)} = \frac{5}{6}.$$

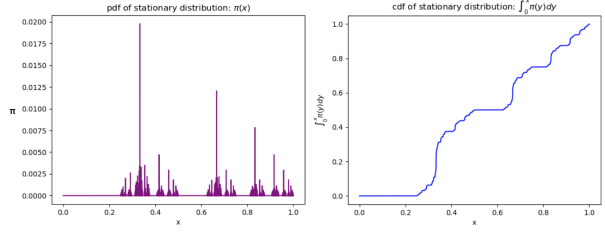


Figure 7: Calculated stationary distribution.

## C.2 Remark: Closed-form unavailable

Ending remark for this Appendix section, and as a complement to the asymptotic analysis of CBB, we provided the following example, where, the closed-form solution of the stationary distribution of the proportion of active arms can only be calculated numerically but not characterized in clean closed-form as the above example.

**Single-Type Base Example 2** Consider a base CBB example with only one type of arm (i.e.,  $M = 1$ ). Let there be  $\rho$  copies of this arm in the scaled setting as  $\rho \rightarrow \infty$ . We drop the index  $i$  for convenience. Suppose there are two contexts,  $k \in \{1, 2\}$ , each occurring with probability  $f_1 = f_2 = 0.5$ . **Transition Probabilities and Rewards.** Let  $\epsilon > 0$ . The transition probabilities and rewards are defined as follows.

**Transition Probabilities and Rewards.** Let  $\epsilon > 0$ . The transition probabilities and rewards are defined as follows.

- **Context 1: Transition probabilities:**

$$\begin{aligned} P^1[s^{t+1} = 1 \mid s = 1, a = 1] &= 1 - \epsilon, \\ P^1[s^{t+1} = 0 \mid s = 1, a = 1] &= \epsilon, \\ P^1[s^{t+1} = 1 \mid s = 1, a = 0] &= 1, \\ P^1[s^{t+1} = 0 \mid s = 1, a = 0] &= 0, \\ P^1[s^{t+1} = 1 \mid s = 0, \forall a = 0, 1] &= \frac{1}{2} \\ P^1[s^{t+1} = 0 \mid s = 0, \forall a = 0, 1] &= \frac{1}{2} \end{aligned}$$

**Rewards:**

$$\begin{aligned} r(s^t = 1, a^t = 1; k = 1) &= 1, \\ r(s^t = 1, a^t = 0; k = 1) &= 0, \\ r(s^t = 0, a^t = 1; k = 1) &= 0, \\ r(s^t = 0, a^t = 0; k = 1) &= 0. \end{aligned}$$

- **Context 2: Transition probabilities:**

$$\begin{aligned} P^2[s^{t+1} = 1 \mid s = 1, a = 1] &= 0, \\ P^2[s^{t+1} = 0 \mid s = 1, a = 1] &= 1, \\ P^2[s^{t+1} = 1 \mid s = 1, a = 0] &= 1, \\ P^2[s^{t+1} = 0 \mid s = 1, a = 0] &= 0, \\ P^2[s^{t+1} = 1 \mid s = 0, \forall a = 0, 1] &= \frac{1}{2} \\ P^2[s^{t+1} = 0 \mid s = 0, \forall a = 0, 1] &= \frac{1}{2} \end{aligned}$$

**Rewards:**

$$\begin{aligned} r(s^t = 1, a^t = 1; k = 2) &= 1 + \epsilon, \\ r(s^t = 1, a^t = 0; k = 2) &= 0, \\ r(s^t = 0, a^t = 1; k = 2) &= 0, \\ r(s^t = 0, a^t = 0; k = 2) &= 0. \end{aligned}$$

**Budget Constraint.** Assume the budget in each round is a fraction of the total number of arms. For concreteness, let the budget be

$$B = \left\lfloor \frac{1}{4} \rho \right\rfloor,$$

so that we may activate at most  $\lfloor \frac{\rho}{4} \rfloor$  arms (out of  $\rho$ ). As  $\rho \rightarrow \infty$ , we can assume without loss of generality that  $B = \frac{\rho}{4}$  is an integer.

The occupancy-measure LP simplifies to

$$\begin{aligned} \max_{\mu, B_k} \quad & \mu(1, 1, 1) + \mu(1, 1, 2) (1 + \epsilon) \\ \text{subject to} \quad & \frac{1}{2} (1 - P[s = 1]) = \epsilon \mu(1, 1, 1) + \mu(1, 1, 2), \\ & \mu(1, 1, k) \leq \frac{1}{2} P[s = 1], \quad \forall k \in \{1, 2\}, \\ & \mu(1, 1, 1) + \mu(1, 1, 2) \leq 0.25 \end{aligned}$$

The optimal solution is  $P^*[s = 1] = 0.5$ ,  $\mu^*(1, 1, 1) = 0$ ,  $\mu^*(1, 1, 2) = 0.25$ . Similarly, COcc would allocate budget so that

$$\begin{aligned} B_1 &= 0, \\ B_2 &= 0.5\rho. \end{aligned}$$

Therefore, from 32 and 33 we obtain for the stationary distribution  $\pi$ :

$$\pi(y) = \begin{cases} 0 & y \in (0, \frac{1}{4}) \\ \frac{1}{2}\pi(\frac{1}{2}) & y = \frac{1}{4} \\ \frac{1}{2}\pi(1 - 2y) + \frac{1}{2}\pi(2y) & y \in (\frac{1}{4}, \frac{1}{2}) \\ \frac{1}{2}\pi(2y - 1) & y \in (\frac{1}{2}, 1]. \end{cases} \quad (34)$$

It doesn't have a clean closed-form solution. But the stationary of proportion of active arms ( $\pi(\cdot)$ ) can be solved numerically, as shown in Figure 7. As shown in Figure 7, for non-trivial probability, the proportion of active arms is less than 0.5—less than the required active arms to pull. The station-

737 any reward can be calculated as

$$\begin{aligned}
& \mathcal{R}^{\text{COcc}} \\
&= \int_0^1 \sum_k f_k r(k) \rho \min(\beta_k, x) \pi(x) dx \\
&= \rho \int_0^1 \frac{1}{2} (1 + \epsilon) \min\left(\frac{1}{2}, x\right) \pi(x) dx \\
&\approx \rho(1 + \epsilon)0.214.
\end{aligned}$$

738 However, notice that the other context  $k = 1$  is almost al-  
739 ways active (it has probability  $p = \epsilon$  of transfer to inactive).  
740 Therefore, if we allocate all budget to it—almost all arms  
741 will be active all the time, and reward of  $r(1) = 1$  can be  
742 accrued at every pull. By back-on-the-envelope calculation,  
743 under this budget allocation (all to context 1) the system gen-  
744 erate (almost) exactly  $\frac{1}{4}$  reward. Therefore, this instance give  
745 an lowerbound of  $0.214/0.25 = 0.856$  impossibility lower-  
746 bound for the LP-induced budgets.

## 747 D Experiment Details: Design and 748 Implementation

### 749 D.1 Low/High Activeness in Synthetic Food 750 RescueCBB

751 We blend two types of synthetic setups to merge and simulate  
752 different dynamics in formulating the food rescue CBB:

#### 753 High Activeness

In the High Activeness instance,  $N$  volunteers and  $K$  re-  
754 gions are randomly positioned on a two-dimensional plane.  
755 Each volunteer and region is associated with a location and  
756 attributes—namely, volunteer activeness, region popularity,  
757 and a historical record  $H_i$  (which, in turn, influences the con-  
758 text probabilities  $f_k$ ). For every volunteer  $i$  and region  $k$ , we  
759 define the pick-up rate as

$$p_{i,k} = \exp\left(\alpha \text{pop}_k - \gamma d(i, k) + \beta \frac{|H_i|}{H_{\max}}\right),$$

754 where

755 -  $\alpha$  is the parameter capturing the influence of region pop-  
756 ularity (with  $\text{pop}_k$  denoting the popularity of region  $k$ ), -  $\gamma$   
757 is the distance sensitivity parameter (with  $d(i, k)$  represent-  
758 ing the distance between volunteer  $i$  and region  $k$ ), -  $\beta$  is the  
759 parameter reflecting volunteer activeness (with  $|H_i|$  being the  
760 size of volunteer  $i$ 's history), and -  $H_{\max}$  is a normalization  
761 constant.

762 Transition dynamics are such that an active volunteer (state  
763  $s = 1$ ) who is notified (action  $a = 1$ ) picks up the task with  
764 probability  $p_{ik}$  and may then become inactive. The immedi-  
765 ate reward for a notification is a function of region popularity  
766 and  $p_{ik}$ .

#### 767 Low Activeness

768 In addition to the High Activeness instance, we define a Low  
769 Activeness instance to capture more challenging dynamics  
770 within the CBB framework. It is motivated by the scenario  
771 that induces the theoretical  $5/6$  inefficiency for COcc in The-  
772 orem 2 (see Appendix C.1 for details).

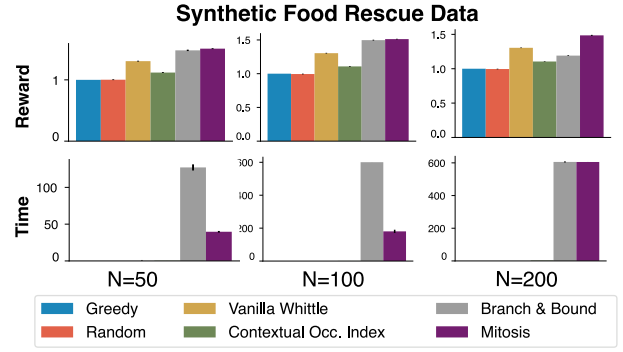


Figure 8: Ablation Experiments on Synthetic Food Rescue Experiments, Varying Number of Volunteers

The  $K$  regions are partitioned into *nasty* regions ( $\mathcal{K}_{\text{nasty}} \subsetneq [K]$ ) and its complement. The nasty regions are adversarially designed such that, for any volunteer  $i$ , the pick-up probabilities  $p_{ik}$  for  $k \in \mathcal{K}_{\text{nasty}}$  are drawn uniformly around a high mean (e.g., centered at 0.95), making these regions very attractive and yielding a high probability of transitioning a volunteer to an inactive state. In contrast, for regions  $k \notin \mathcal{K}_{\text{nasty}}$  (the “cheap” regions), the transition probabilities are concentrated around a low mean (e.g., centered at 0.05). Recovery probabilities  $q_i$  for volunteers are generated around a prescribed mean (e.g., 0.2). Moreover, the reward structure is modified so that notifications in nasty regions yield a slightly elevated immediate reward (e.g.,  $1 + \epsilon$ ) to reflect their allure despite the adverse long-term effect. This construction presents a challenge for COcc theoretically, as shown in the proof of Theorem 2 in its proof in Appendix C.1.

#### Blended Instance

Finally, we construct a *Blended Instance* that merges High Activeness and Low Activeness dynamics. A fraction  $\rho_{\text{Abundance}} \in [0, 1]$  (termed the *sensitivity ratio*) of the  $N$  volunteers is designated to follow Low Activeness dynamics, while the remaining  $N - N_{\text{active}}$  volunteers follow High Activeness dynamics. Formally, we set

$$N_{\text{active}} = \lfloor \rho_{\text{Abundance}} N \rfloor,$$

and generate two independent instances over the same set of  $K$  regions:

- (i) A *high activity instance* with  $N_{\text{active}}$  volunteers. The transition dynamics and rewards are constructed as described in Section D.1
- (ii) A *low activity instance* with  $N - N_{\text{active}}$  volunteers, constructed as described in Section D.1.

## D.2 Ablation Experiments on Synthetic Food Rescue Instance

Below, we summarize the ablation study results on synthetic data, where we systematically vary the number of volunteers ( $N$ ), the number of regions ( $K$ ), and the budget ( $B$ ).

- **Varying number of volunteers for  $N = 50, 100, 200$ , fix  $K = 3$  regions and budget be 5% number of volunteers (Figure 8):** As  $N$  increases, Mitosis (purple)

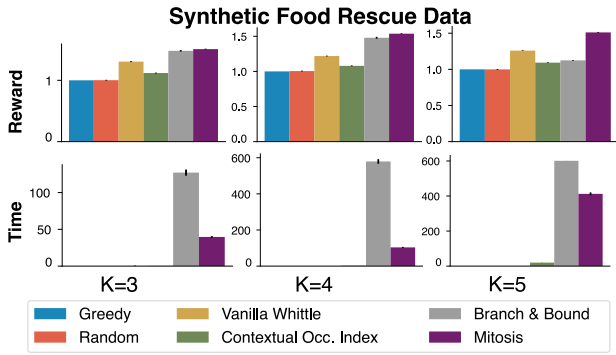


Figure 9: Ablation Experiments on Synthetic Food Rescue Experiments, Varying Number of Contexts

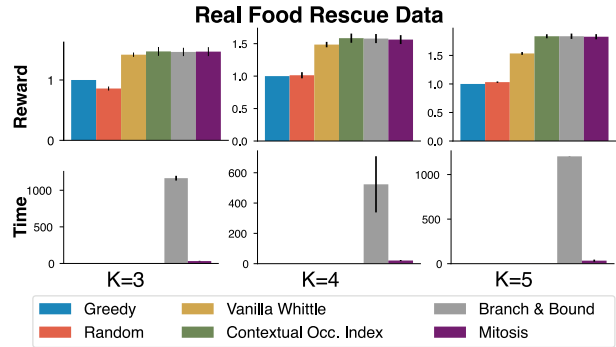


Figure 12: Ablation Experiments on Real Food Rescue Experiments, Varying Number of Contexts

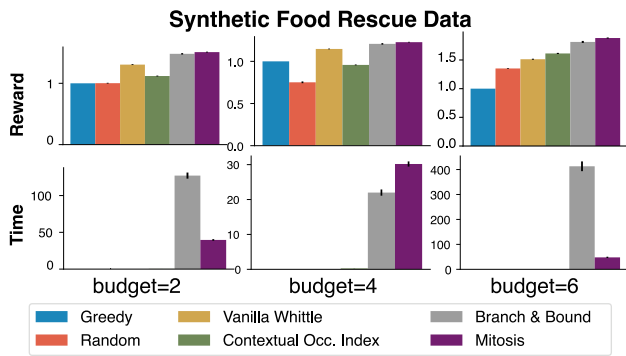


Figure 10: Ablation Experiments on Synthetic Food Rescue Experiments, Varying Budget

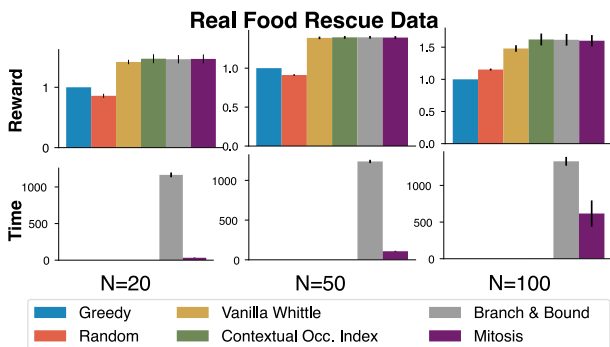


Figure 11: Ablation Experiments on Real Food Rescue Experiments, Varying Number of Volunteers

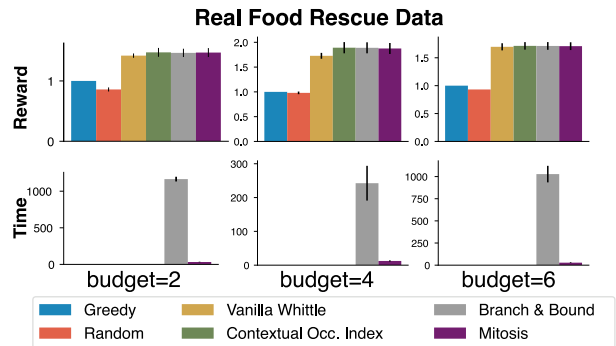


Figure 13: Ablation Experiments on Synthetic Food Rescue Experiments, Varying Budget



consistently leads in reward and remains much faster than Branch And Bound (gray). Note that in  $N = 200$  both Branch And Bound and Mitosis reach the time limit (600s) and is terminated, but still within the same time limit, the Mitosis’s solution is more than that of Branch And Bound’s, demonstrating that Mitosis is much faster. COcc (green) still lags in reward, indicating it does not fully exploit the increased volunteer pool.

- **Varying number of regions for  $K = 3, 4, 5$ , fix number of volunteers  $N = 50$ , budget  $B = 5$  (Figure 9):** With more regions, the search space for budget increases exponentially. Branch And Bound maintains a slight reward edge but at a steep runtime cost, it times out already at  $k = 4$ . Mitosis remains best and is faster compared to Branch And Bound. COcc gains some benefit but continues to underperform compared to the optimal.
- **Varying budget  $B = 2, 4, 6$ , fix volunteers  $N = 50$ , regions  $K = 3$  (Figure 10):** Increasing  $B$  allows more notifications, boosting Mitosis substantially while also helping COcc close some of the gap. Once again, Branch And Bound yields top-tier rewards but incurs much higher computation time.

### D.3 Ablation Experiments on Real Food Rescue Data

Similar as synthetic data’s ablations, we systematically vary the number of volunteers ( $N$ ), the number of regions ( $K$ ), and the budget ( $B$ ) of CBB constructed on real food rescue data. Results are shown in

- Figure 11: changing  $N = 20, 50, 100$  while maintain number of regions  $K = 3$ , budget  $B = 2$ .
- Figure 12: changing  $K = 3, 4, 5$  while maintaining number of regions  $N = 20$ , budget  $B = 2$ .
- Figure 13: changing  $B = 2, 4, 6$  while maintaining number of volunteers  $N = 20$ , number of regions  $K = 3$ .

As the scale of the instance increases ( $N, K$  or  $B$  increases), Vanilla Whittle performance grows worse compared to COcc, Branch And Bound, Mitosis which they perform similarly. This shows that (i) when the scale of the problem increase, it is necessary to introduce context-aware policies to reach optimal performance (ii) in application, COcc is sufficient for near-optimal performance. Mitosis guarantees optimality and is significantly faster than Branch And Bound.

## E Generalizability to Other Application Areas

While we ground our methodological work in food rescue volunteer engagement, the Contextual Budget Bandit model and its algorithms are applicable to a variety of domains. In this section, we describe a few of these applications.

**Digital agriculture** Smallholder farmers in the global south feed their countries yet are vulnerable to climate change and market fluctuation. Agriculture chatbots are a promising direction to empower smallholder farmers, as evidenced, for example, in an NSF report [Guérin *et al.*, 2024]. In collaboration with Organization X, we have a chatbot which sends

---

### Algorithm 2 Branch And Bound

---

**Input:** Feasible Region  $\mathcal{B}_0, \mathbb{L}^P$ , Oracle

**Output:** Budget Allocation  $\vec{B}^*$

```

1: Initialize:  $R^{\text{OPT}} \leftarrow -\infty, \vec{B}^{\text{OPT}} \leftarrow \text{None}, \text{Queue } Q \leftarrow \{\mathcal{B}_0\}$ .
2: while  $Q \neq \emptyset$  do
3:   Dequeue  $\mathcal{B} \leftarrow Q.\text{pop}()$ .
4:   if  $\mathbb{L}^P(\mathcal{B}) < R^{\text{OPT}}$  then
5:     continue.  $\{\text{prune } \mathcal{B}\}$ .
6:   end if
7:    $\vec{B}^* \leftarrow \vec{B}^{\mathbb{L}^P}(\mathcal{B}) \{\text{most promising } \vec{B} \in \mathcal{B}\}$ 
8:   if Oracle( $\vec{B}^*$ )  $> L^*$  then
9:     Update  $L^* \leftarrow \text{Oracle}(\vec{B}^*)$  and  $\vec{B}^{\text{OPT}} \leftarrow \vec{B}^*$ .
10:  end if
11:  Branch: Partition  $\mathcal{B} = \mathcal{B}_1 \cup \mathcal{B}_2$ 
12:   $Q \leftarrow Q \cup \{\mathcal{B}_1, \mathcal{B}_2\}$ .
13: end while
14: return  $\vec{B}^*$ .

```

---

out regular nudges about farming practices to over 10,000 farmers in India, Kenya, and Nigeria. However, nudges of different topics have different conversion rates. Pest control tips during the pest season address an urgent problem, usually resulting in high conversion rates. Meanwhile, watering tips are preventive measures, which often have lower conversion rates by the farmers. Thus, when planning the engagement strategy over time, one would want to assign different nudging budgets to different topics of nudges, and model it as a CBB. Each farmer is an arm. At each time step, we have a nudge topic as context, and we decide on a budget of how many farmers to notify and the arm selection of who to notify. Rewards are determined based on farmer’s engagement response.

**Peer review** In peer review, journals select reviewers for submissions where selection impacts future reviewer availability [Payan and Zick, 2021]. For a given paper, the goal is to select a subset of available reviewers with the relevant subject-matter expertise. However, submissions differ from one another. For example, submissions that are extra long, that involves heavy theoretical analysis, or that do not study the trendy topics might have lower chance of getting reviewers to agree to review. Thus, when the editor plans reviewing invitations over time, they would want to send different numbers of invitations to different kinds of submissions, and model it as a CBB. Each potential reviewer is an arm. At each time step, we have a submission type as context, and we decide on a budget of how many potential reviewers to reach out to, and the arm selection of who to reach out to. Rewards are determined based on the reviewers’ response.

## F Pseudocode for Branch And Bound Algorithm

859  
860  
861  
862  
863  
864  
865  
866  
867  
868  
869  
870  
871  
872  
873  
874  
875  
876  
877  
878  
879  
880  
881  
882  
883  
884  
885  
886  
887  
888  
889  
890

## 891 G No-Regret Guarantee for the Mitosis 892 Algorithm

893 In the MAB framework each arm represents a candidate bud-  
894 get allocation  $\vec{B}$  from the feasible set

$$\mathcal{B}_0 \triangleq \left\{ \vec{B} \in \mathbb{N}^K : \sum_{k=1}^K B_k \leq B \right\}.$$

895 Pulling an arm  $\vec{B}$  corresponds to calling the fast oracle  
896 Oracle<sub>small</sub>( $\vec{B}$ ) (with epoch = 1) which returns a noisy es-  
897 timate of the reward  $\mu(\vec{B})$ . Thus, by running a Multi-Armed  
898 Bandit (MAB) algorithm over the arms  $\vec{B} \in \mathcal{B}_0$  we aim to se-  
899 lect the arm with the highest expected reward without having  
900 to estimate  $\mu(\vec{B})$  for every  $\vec{B}$ .

901 **Definition** (Reward Regret). Let

$$\mu^* \triangleq \max_{\vec{B} \in \mathcal{B}_0} \mu(\vec{B})$$

902 and denote by  $\vec{B}_t$  the budget allocation (arm) chosen at time  
903  $t$ . Then the instantaneous regret at time  $t$  is

$$\Delta_t \triangleq \mu^* - \mu(\vec{B}_t),$$

904 and the cumulative (reward) regret over a time horizon  $T$  is  
905 defined as

$$R(T) \triangleq \sum_{t=1}^T \Delta_t = \sum_{t=1}^T (\mu^* - \mu(\vec{B}_t)).$$

906 The goal is to design an algorithm whose cumulative regret  
907 grows sublinearly in  $T$ ; that is,  $\frac{R(T)}{T} \rightarrow 0$  as  $T \rightarrow \infty$ . In our  
908 setting, the optimal budget allocation  $\vec{B}^*$  (with  $\mu(\vec{B}^*) = \mu^*$ )  
909 will be identified as  $T$  increases.

**Theorem 3.** [No-Regret of the Mitosis Algorithm] Let  $\mathcal{A}$  de-  
note the set of arms that have been pulled. After running the  
algorithm for  $T$  rounds, the cumulative regret

$$R(T) \triangleq \sum_{t=1}^T (\mu^* - \mu_t)$$

satisfies

$$R(T) = \sum_{\vec{B} \in \mathcal{A}} \mathbb{E}[N_T(\vec{B})] \Delta(\vec{B}) = O\left(\sum_{\vec{B} \in \mathcal{A}} \frac{\log T}{\Delta(\vec{B})}\right),$$

910 which matches the UCB1 regret bound.

911 *Proof.* The proof is built on the classical UCB1 analysis of  
912 Auer *et al.* [2002]. In the Mitosis Algorithm (Algorithm 1),  
913 each arm  $\vec{B}$  is initialized with its upperbound  $\text{LP}(\vec{B})$ . The  
914 algorithm maintains two types of arms:

915 • **Unpromising arms:** Arms that are encapsulated in  
916 StemArm, who has not yet been pulled. Their index is  
917 given by  $\text{LP}(\vec{B})$ .

• **Candidate arms:** Arms that have been pulled at least  
once. For these, the UCB index at time  $t$  is defined as

$$I_t(\vec{B}) = \hat{\mu}_t(\vec{B}) + c\sqrt{\frac{\log t}{N_t(\vec{B})}},$$

918 where  $\hat{\mu}_t(\vec{B})$  is the empirical mean,  $N_t(\vec{B})$  is the num-  
919 ber of pulls, and  $c > 0$  is a constant.

920 The algorithm runs for  $T$  rounds; by the end, let  $\mathcal{A}$  denote  
921 the final set of candidate arms. We consider two cases based  
922 on the location of the optimal arm  $\vec{B}^*$ .

923 *Case 1:*  $\vec{B}^* \in \mathcal{A}$ . In this case, the optimal arm has been  
924 pulled at least once. Therefore, the candidate arms  $\mathcal{A}$  form a  
925 sub-MAB instance where we can directly apply UCB1's re-  
926 gret bound on; the arms in StemArm are not pulled anyway,  
927 so they do not contribute to regret. Standard UCB1 analy-  
928 sis (using a peeling argument and concentration inequalities,  
929 see Auer *et al.* [2002]) shows that the expected pulls on any  
930 suboptimal arms, denoted by  $N_t(\vec{B})$ , satisfy

$$\mathbb{E}[N_t(\vec{B})] = O\left(\frac{\log t}{\Delta(\vec{B})^2}\right). \quad (35)$$

Thus, the regret incurred by arms in  $\mathcal{A}$  is

$$R(T) = \sum_{\vec{B} \in \mathcal{A}} \mathbb{E}[N_T(\vec{B})] \Delta(\vec{B}) = O\left(\sum_{\vec{B} \in \mathcal{A}} \frac{\log T}{\Delta(\vec{B})}\right).$$

931 *Case 2:*  $\vec{B}^* \notin \mathcal{A}$ . We prove that this case will never hap-  
932 pen by contradiction. In other words, the optimal arm that  
933 represents the optimal budget solution for CBB will also be  
934 budded out by the StemArm in Mitosis algorithm, as the time  
935 horizon is sufficiently large. 936

Let  $\vec{B}^{2nd} := \arg \max_{a \in \mathcal{A}} \mu(a)$  be the arm with the highest  
mean in the candidate arms. Since the number of pulls for all  
other suboptimal arms satisfies (35), the number of pulls for  
 $\vec{B}^{2nd}$  grows linearly with  $t$ :

$$\mathbb{E}[N_T(\vec{B}^{2nd})] = T - O(\log T).$$

Since  $\vec{B}^* \in \text{StemArm}$ , by the end of the algorithm, the  
StemArm's index ( $\text{LP}(\text{StemArm})$ ) is smaller than the UCB in-  
dex of  $\vec{B}^{2nd}$ . Since  $\vec{B}^* \in \text{StemArm}$ , we have

$$\text{LP}(\text{StemArm}) \geq \text{LP}(\vec{B}^*) \geq \mu(\vec{B}^*).$$

937 then, the event that the suboptimal arm  $\vec{B}^{2nd}$ 's UCB index  
938 be strictly greater than the optimal arm's mean  $\mu(\vec{B}^*)$ : for  
939  $\mu(\vec{B}^*) > \hat{\mu}_T(\vec{B}^{2nd})$ ,

$$\Pr \left[ I_T(\vec{B}^{2nd}) \geq \mu(\vec{B}^*) \right] \quad (36)$$

$$= \Pr \left[ \hat{\mu}_T(\vec{B}^{2nd}) + c\sqrt{\frac{\log(\mathcal{O}(T))}{N_T(\vec{B}^{2nd})}} \geq \mu(\vec{B}^*) \right] \quad (37)$$

$$\leq \exp \left\{ -\frac{\mathcal{O}(T)(\mu(\vec{B}^{2nd}) - \mu(\vec{B}^*))^2}{c'} \right\} \quad (38)$$

$$(39)$$

The probability declines exponentially. Since the probability of the event in Case 2 decays exponentially with  $T$ , its contribution to the overall expected regret is negligible compared to the regret in Case 1. In other words, with probability tending to one as  $T \rightarrow \infty$ , the optimal arm  $\vec{B}^*$  is eventually pulled and becomes a candidate arm. Therefore, the overall expected regret of the Mitosis algorithm is dominated by the regret incurred in Case 1, and we have

$$R(T) = \mathcal{O}\left(\sum_{\vec{B} \in \mathcal{A}} \frac{\log T}{\Delta(\vec{B})}\right).$$

940 Overall the regret of Mitosis is controlled by the classical  
941 UCB1 guarantee, up to a constant factor, and hence the algo-  
942 rithm achieves near-optimal performance. This completes the  
943 proof.

944 □